IN-36
185516
p-44
451679

NASA Contractor Report 191525

NOVEL Co:MgF_2 LIDAR FOR AEROSOL PROFILER

M. A. Acharekar

SCHWARTZ ELECTRO-OPTICS, INC.
3404 N. Orange Blossom Trail,
Orlando, FL 32804

Contract NAS1-19300
September 1993

National Aeronautics and
Space Administration

Langley Research Center
Hampton, Virginia 23681-0001

PREFACE

This was a Small Business Innovation Research (SBIR) Phase II program from NASA, Langley Research Center, (LaRC), Hampton, VA 23665 conducted at Schwartz Electro-Optics, (SEO), Orlando, FL 32818 under contract #NAS1-19300. Dr. Madhu Acharekar was the Principal Investigator (PI) for the program. The NASA technical contract monitor was Dr. David Winker at NASA/LaRC. The laser hardware was fabricated at SEO, Solid State Laser Division under leadership of Mr. Edward Adamkiewicz. The lidar experimental set-up and data was collected by Dr. Dennis Killinger at University of South Florida (USF) under a subcontract. This is the final report for the contract.

TABLE OF CONTENTS

LIST OF FIGURES

LIST OF FIGURES (cont.)

LIST OF TABLES

1.0 INTRODUCTION

Schwartz Electro-Optics, Inc. (SEO) conducted this program on the "Novel $Co:MgF_2$ Lidar for Aerosol Profiler" under a small business innovative research (SBIR) Phase II award (Contract No. NAS1-19300) from NASA Langley Research Center. SEO manufactured the $Co:MgF_2$ laser in a **Laser 1-2-3** housing and also provided a Q-switched CTH:YAG, CTH:YSGG, CT:YAG, and Er:Glass modules for the laser. SEO Consultant Dr. D. Killinger at the University of South Florida (USF), Tampa, Florida assembled a lidar using the laser and collected the data.

There has been a requirement for eye-safe, efficient, reliable, solid state lidar systems in order to measure and monitor atmospheric density profiles and aerosol concentrations at ranges up to 10's of kilometers away. In this development program, the usefulness of newly emerging solid state lasers which operate in the eye-safe spectral region (wavelength > 1.4 μm) were evaluated and their capabilities in lidar systems for obtaining atmospheric aerosol profiles was explored.

Several candidate lasers have recently been developed which show possible potential for such applications, and include the (1) new, room temperature tunable $Co:MgF_2$ laser, (2) 2.1 μm Ho:YAG laser, (3) 2.01 μm Tm:YAG laser, and (4) 1.54 μm Er:Glass laser. Of these, the first two are the most technically advanced and are being commercially offered by private industry. In addition to the above candidate laser sources, recent advances in new, solid state InGaAsP photodetectors in the 1 - 2.6 μm spectral range have also helped to spur lidar development interest in this eye-safe wavelength range.

The research conducted in this program involves building upon the initial Phase I study which demonstrated the potential usefulness of the new, room temperature $Co:MgF_2$ laser for atmospheric lidar studies. In the Phase I study, the feasibility of a direct detection $Co:MgF_2$ lidar system was demonstrated. Some additional experiments were conducted in order to also compare the $Co:MgF_2$ results with other solid state Lidar systems, specifically Ho:YAG and Nd:YAG lidars. The Phase II study indicated that the $Co:MgF_2$ Lidar works well, but is of moderate power (50 mJ/pulse) and appears to be better suited for a much needed experimental survey of the optimal aerosol lidar wavelength over the 1.7 - 2.5 μm range. However, at the present time the Ho lidar offers higher power (250 mJ/pulse) than that of the $Co:MgF_2$. Thus, Ho:YAG and Ho:YSGG lidar data were collected for this program.

1.1 LIDAR FOR AEROSOL PROFILER

Because of the large number of different solid state lidar programs now being conducted (by NASA, ONR, DoD, etc.), it is informative to give the relationship of one program to another. In the case of the present Phase II SBIR for $Co:MgF_2$ program, a comparison has to be made to past $Co:MgF_2$ and Ho:YAG lidar studies, as well as future studies which need to be done. The outline given below will clearly show the work performed in the Phase II study:

1.1.1 PREVIOUS WORK

1) Liquid N_2 Cooled, Low Power $Co:MgF_2$ Lidar Research: The $Co:MgF_2$ laser has already been used in a Lidar system to detect atmospheric aerosols at ranges up to 3 km away. The $Co:MgF_2$ laser crystal was Q-switched, but had to be cooled with liquid nitrogen, and was only tunable from 1.5 - 1.9 μm (ref. 1).

2) Low Power 2.1 μm Ho:YAG Lidar Research: A low power (10 mJ/pulse) Ho:YAG laser was used in a Lidar system for the first time and atmospheric aerosol returns were measured at ranges out to 2 km (ref. 2). The Ho:YAG laser available for this research had a spinning mirror Q-switch and produced low energy pulses. The work was conducted by SEO under a Phase I SBIR program from the Department of Commerce. Since then several Ho Lidars have been reported (ref. 3-5)

1.1.2 CURRENT WORK

1) NASA Phase I & II SBIR Room Temperature $Co:MgF_2$ Lidar: The new, room temperature $Co:MgF_2$ laser has been used in the present NASA Phase I & II SBIR study to provide preliminary information of its usefulness as an aerosol lidar profiler.

2) Moderate Power Ho:YAG Lidar Research: SEO recently developed a Ho lidar under a Department of Commerce Contract No. 50-DKNE-8-00126 with USF. The Ho Lidar system at USF was upgraded to include this higher power, Q-switched laser design.

3) High Power Nd:YAG Lidar Research: A high power (1 J/pulse) short pulse (8 ns) Nd:YAG lidar has been developed at USF and is being used to study both direct detection and heterodyne detection of solid state lidar returns. SEO is also conducting work under Contract No. N00014-90-C-0013 funded by the Office of Naval Research (ONR) on a one micron heterodyne system.

1.2 SUMMARY

The technical objectives for the Phase II program, outlined in section 2.0, and the results are described in section 3.0 of this report. This was a complex program involving several groups (SEO, Research and Solid State Laser Divisions, University of South Florida). However, SEO believes that this innovative research resulted in the development of a $Co:MgF_2$ laser suitable not only for lidar but also for medical applications. In addition, substantial new data have been obtained on use of Ho laser for atmospheric studies.

The overall goal of the SBIR Phase II program was to develop a high-power, eye-safe, solid-state laser that could be used in a lidar system for atmospheric aerosol. The overall program was conducted in two parts: SEO was the prime contractor, and had the responsibility to design and construct the solid state laser system; several different laser sources were considered, and the best or optimal laser chosen for further extensive testing. A subcontract was then performed by the Univ. of So. Florida to test these lasers extensively and to use them in a lidar system.

A high power, multi-module, solid state laser was developed by SEO and studied to determine the optimal high-power eye-safe laser source for atmospheric lidar applications. Under this program, SEO developed and constructed a variety of flashlamp pumped solid-state lasers (Co:MgF_2 with 1.3 μm Nd:YAG pump, Ho:YSGG, Ho:YAG, and Tm:YAG) which were tried as potential candidates for atmospheric lidar applications. SEO developed and tested these different lasers (in conjunction with USF) for their utility as a lidar source. After about a year of testing, it was determined that the optimal laser choice was the 2.1 μm Ho:YAG laser. This laser was delivered to USF in May, 1992 and lidar tests were initiated. The basic findings for the inter-comparison were:

Co:MgF_2 laser: High output power in the non-Q-switched mode. However, significant laser cavity mirror damage was experienced when the laser was Q-switched at power levels greater than 50 mJ/pulse.

Ho:YAG laser: High output power in normal mode; limited to 300 mJ for Q-switched (but half of laser power is in a long tail); multiple wavelength operation (OK for aerosol lidar).

Ho:YSGG laser: Lower in output power than Ho:YAG, and no multiple wavelength problems.

Tm:YAG/YLF laser: Low laser gain system more suited for CW operation. However, it would have significant utility if it could be diode laser pumped.

Er:Glass laser: High threshold system at room temperature; some significant up-conversion problems.

2.0 TECHNICAL OBJECTIVES

The technical objectives of this Phase II SBIR study as originally listed in the proposal were:

- Design, construct, and test a high power, eye safe, solid state lidar for profiling atmospheric aerosol in a wavelength range near 2 micron.

- In addition to a $Co:MgF_2$ laser, several candidate lasers (Ho, Tm, and Er) will evaluated during the program.

- All the lasers and sub-assemblies developed during the program will be delivered to NASA, Langley Research Center.

All of the above objectives were accomplished during the Phase II program. In addition, the results of this study involving Ho lidar systems are summarized in order to best advise the future lidar activities using the laser.

The tasks performed during the program are listed below:

1. Enhancement of $Co:MgF_2$ Laser

2. Production of High Power Ho Laser with Er and Tm Modules for SEO,s Laser 1-2-3

3. Aerosol Lidar Tests Using a High Power Ho Laser Source

4. Wavelength Survey of Lidar Back-scatter Coefficient Using Moderate Power $Co:MgF_2$

5. Deliver and install Laboratory Breadboard Aerosol Profiler Lidar components to NASA

Tasks 1 and 2 were accomplished during the first year of the program and the Tasks 3 and 4 during the second year of the program. Tasks 1 and 2 were performed by SEO, Tasks 3 and 4 by USF, and Task 5 was performed jointly by SEO and USF.

3.0 RESEARCH RESULTS

FIRST YEAR OF PHASE II PROGRAM

3.1 ENHANCEMENT OF $Co:MgF_2$ LASER

The Phase I study showed that the commercially available room temperature non Q-switched, moderate power (20 mJ/pulse) $Co:MgF_2$ laser performed well as a lidar source and that enhanced performance should be obtainable through modifications to the laser design. These modifications include adding an A/O Q-switch and a more refined 3 element birefringent tuning filter to the laser cavity. These modifications were straight forward and based on using SEO's **Laser 1-2-3** also as optical bed for $Co:MgF_2$ laser. The design fabrication work was completed within the first six months of the program.

The room temperature $Co:MgF_2$ laser was enhanced to include Q-switching and wide tunability. The design of the new laser is shown in Figure 1. The tuning data for the laser are shown in Figure 2. Q-switching the $Co:MgF_2$ laser was not successful. An acousto-optical (AO) Q-switch was used. For the wavelength range of 1.75 - 2.5 μm, TeO_2 material was selected due to its high transmission in the near IR wavelength. An optical schematic for the Q-switch is shown in Figure 3. The Q-switch can be also used for Ho, Tm, and Er lasers. The TeO_2 material requires only 10 watts of RF power. Thus, a reduction in RF power supply size is possible. However, two TeO_2 cells were damaged during the Q-switch tests. The typical normal mode pulse is shown in Figure 4. Typically, five distinct relaxation oscillation spikes are observed. The first pulse in the train was estimated to contain 20 mJ energy in 100 ns. The use of this laser for lidar application utilized these pulses, due to relaxation oscillation.

3.2 HIGH POWER Ho LASER WITH Tm AND Er MODULES

3.2.1 NORMAL MODE

A High Power version of the Model **Laser 1-2-3** was manufactured by SEO and tested using interchangeable Er or Tm laser Rods. The laser utilizes a 1 m long optical bed to mount the resonator components. The laser power supply was designed to provide a repetition rate of 0.1-30 pulses per second and a flashlamp pulse width adjustable from 100 to 700 μs. The pump cavity consisted of a polished silver elliptical reflector, a 5 mm by 75 mm long laser rod and a 450 torr xenon gas filled flashlamp. The flashlamp and the laser rod were cooled by a refrigerated closed loop circulating water. It may be noted that the experimental data collected for CTH:YAG indicated that with a flashlamp pulse width between 500-600 μs, the best efficiency for the material was possible. Also, with the coolant water temperature at 10-12 ^{0}C this material provides a higher output energy. At lower coolant temperature a dry air purge is required to avoid condensation on the laser rod ends.

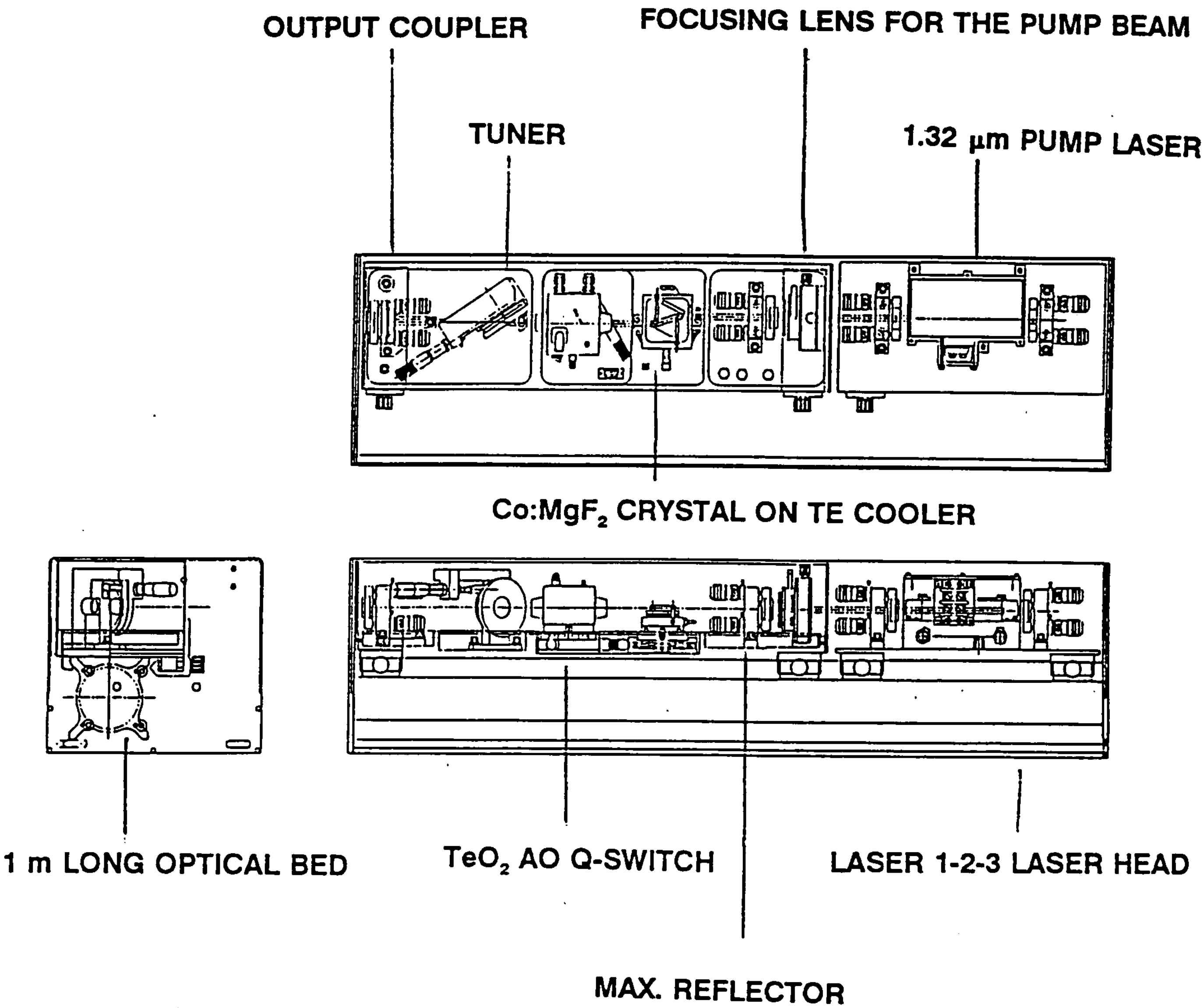

FIGURE 1: ROOM TEMPERATURE Co:MgF_2 LASER

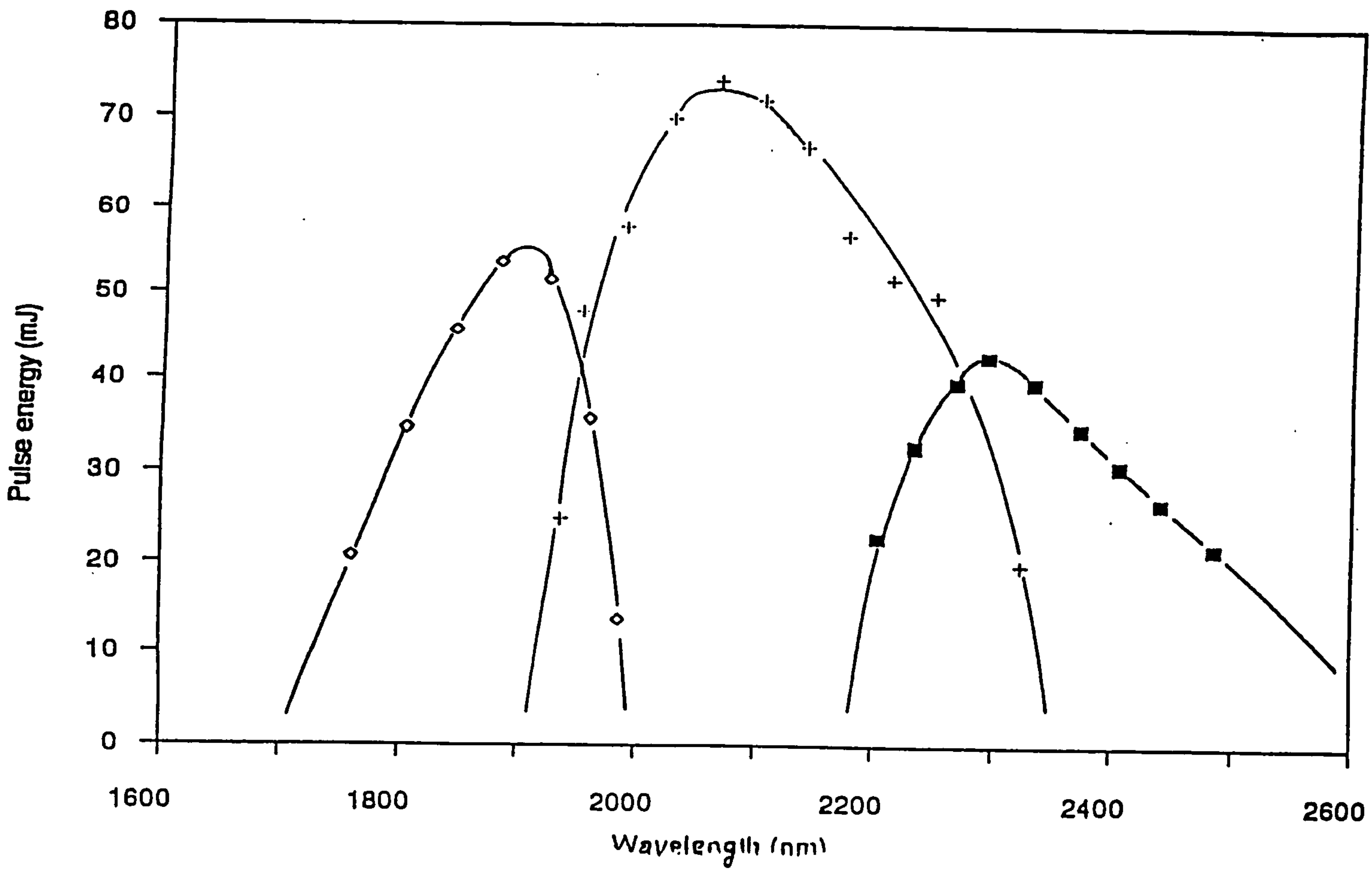

Data collected at SEO, Research Division using SEO R&D funding.

FIGURE 2: TUNING CURVE FOR $Co:MgF_2$ LASER

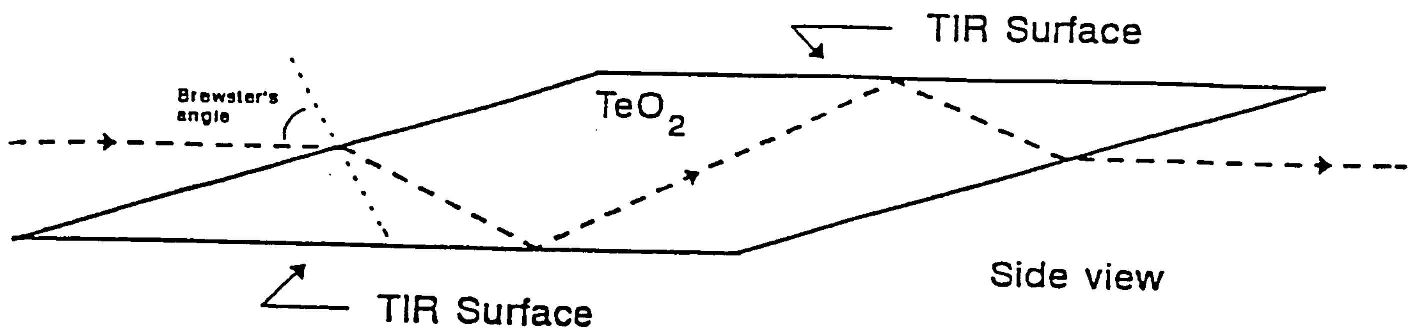

FIGURE 3: OPTICAL SCHEMATIC OF THE ZIG-ZAG SLAB Q-SWITCH

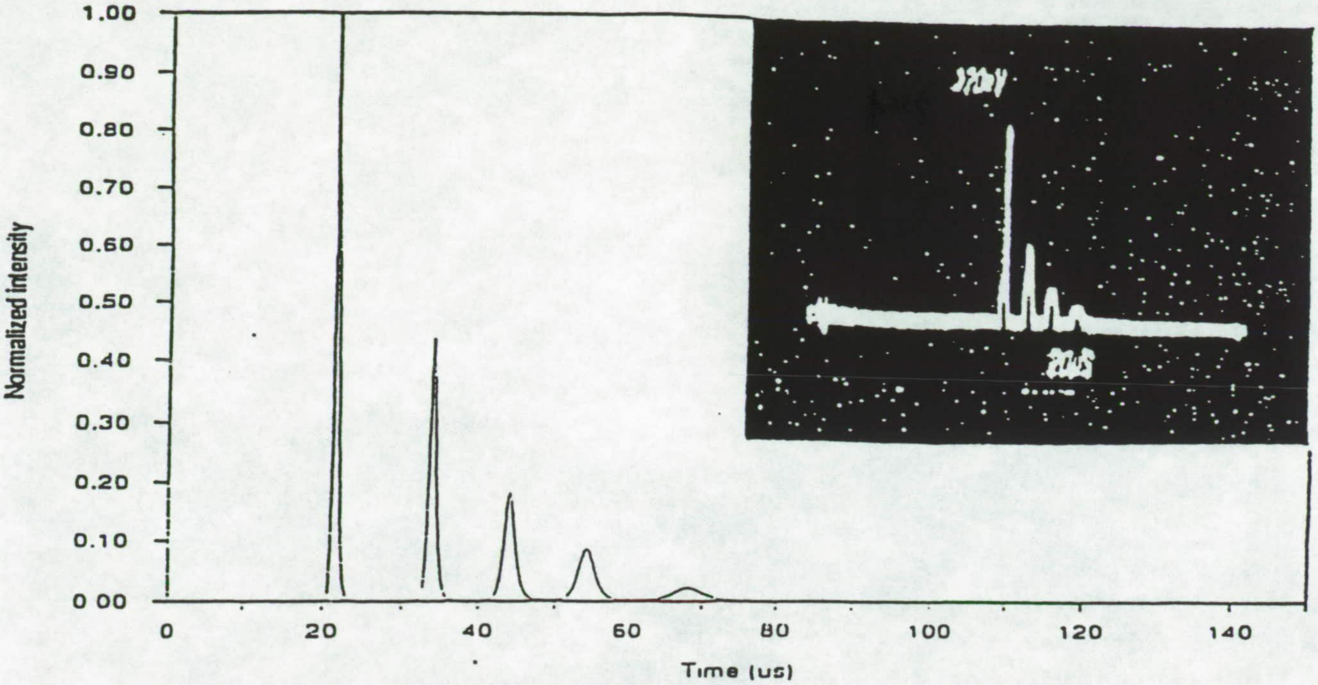

Above Data collected at SEO, Research Division using SEO R&D funding.

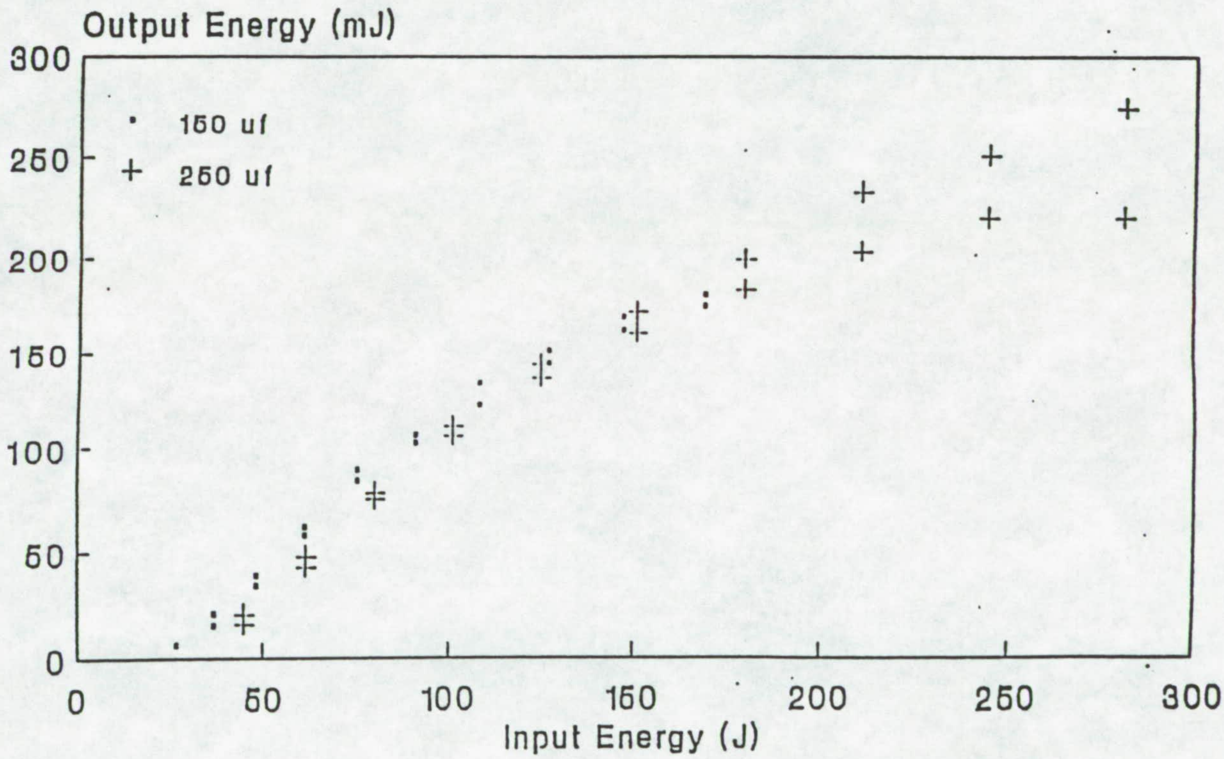

2 Hz Repetition rate
50 % OC @ 1.32, 98% OC @ 2.0
November 27, 1991, File:CO_W_TE.CHT

FIGURE 4: Co:MgF_2 LASER NORMAL MODE OUTPUT

Initially, comparison data was obtained for a CTH:YAG and CTH:YSGG laser rod. In Figure 5, input versus output characteristics for a 5 mm diameter by 75 mm long laser rod is shown. For an Er:Glass laser rod a significantly longer flashlamp pulse is required. The normal mode data obtained for an Er:Glass laser is shown in Figure 6. The data were collected using water coolant and a nitrogen gas purge. The liquid coolant provided poor efficiency as compared to the nitrogen purge.

3.2.2 Q-SWITCH MODE

SEO selected an acousto-optical (AO) Q-switch for this system. The approach was based on a similar system recently developed and tested by SEO and delivered to the USF lidar Laboratory on a program funded by the Florida High Technology Council (FHTC). Therefore, the approach was considered low risk. However, two major improvements were provided in the laser developed for NASA. (1) The Q-switch used for the FHTC program used Suprasil-WF with end surfaces normal to the laser beam and antireflection (AR) coated. These AR coatings damaged at energy levels above 150 mJ/p. As a result, the end surfaces were cut near Brewster's angle for the NASA program. It may be noted that this Q-switch was not the zig-zag slab approach which was used for TeO_2. Instead an off-set approach was used. (2) The second improvement was in the RF driver. In order to obtain higher hold-off, the RF power supply power was increased from 50 W to 100 W. A hold-off of 600 mJ was possible using this increased RF power. Secondly, in order to suppress double pulsing, a window in the RF drive was provided. This window was adjustable from 1-200 μs duration. The laser flashlamp input, RF drive voltage with the window, and Q-switched laser output is shown in Figure 7.

The Q-switched output data for 6.3mm diameter by 75mm long CT:YAG and CTH:YAG are compared in Figure 8. The input versus output characteristic for the 6.3mm diameter by 100mm long CTH:YAG is plotted in Figure 9. It may be noted that as the input energy was increased, not only did the output energy increase, but a decrease in pulse width was observed. At an output energy level of 300 mJ/p, a pulse length of 50 ns (Figure 10) was observed.

The laser design was modular with the capability of operating at 1.54 μm with an Er laser rod or at 2.01 μm with a Tm rod. The Ho, Tm and Er laser cavities are the same with common A/O Q-switches and similar optical components. The Brewster's angle cut Q-switch can be used at these multiple wavelengths. The time required to switch from the Ho laser module to the Er or Tm laser module is under 20 minutes. In Table I, the Q-switch performance is summarized.

TABLE I
COMPARISON OF Q-SWITCHED LASER OUTPUT

TYPE OF LASER	Q-SWITCHED OUTPUT
Er:Glass	> 10 mJ
CT:YAG	125 mJ
CTH:YAG	350 mJ

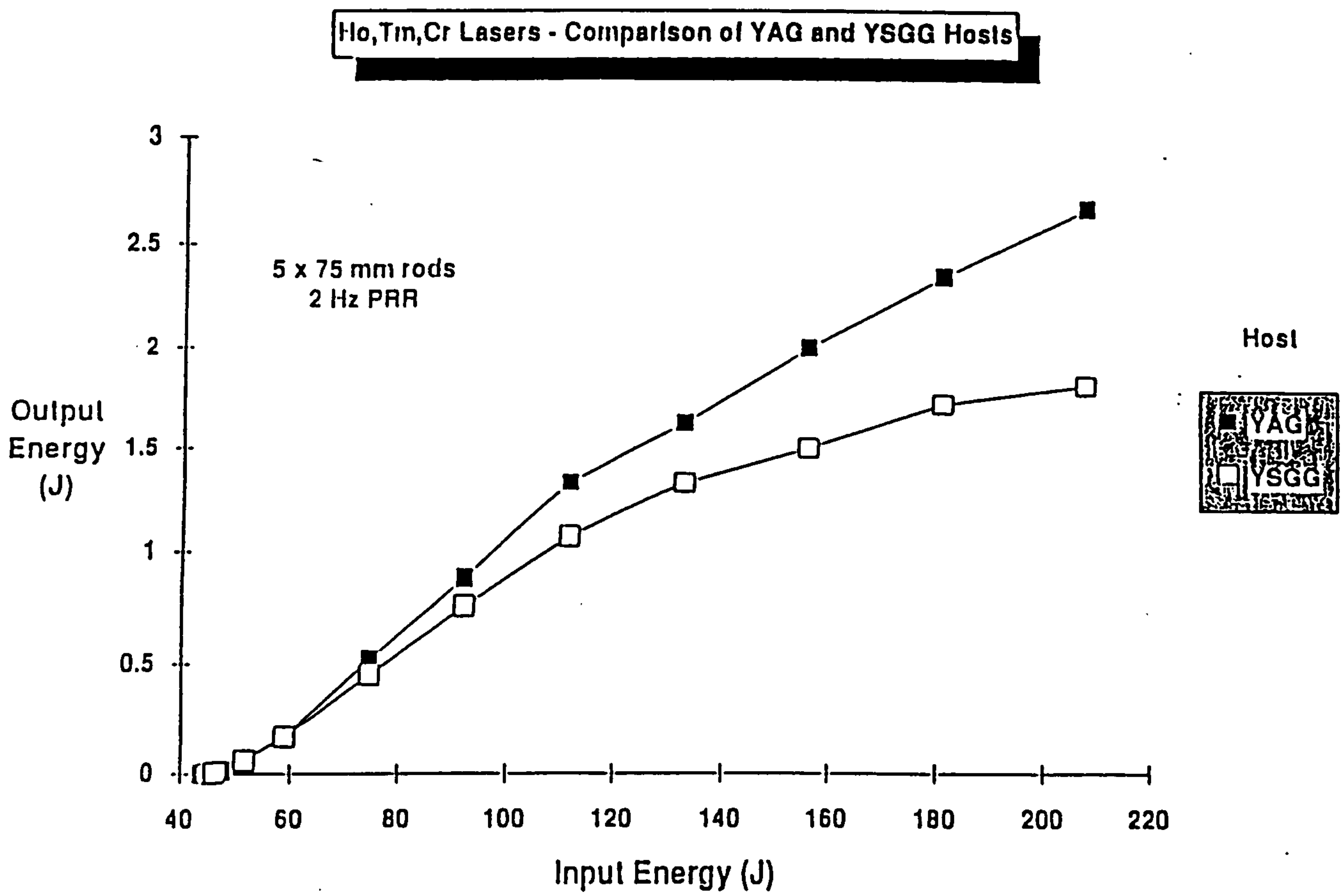

Data collected at SEO, Research Division on another program.

FIGURE 5: COMPARISON OF YAG AND YSGG HOST FOR Ho, Cr, Tm LASER

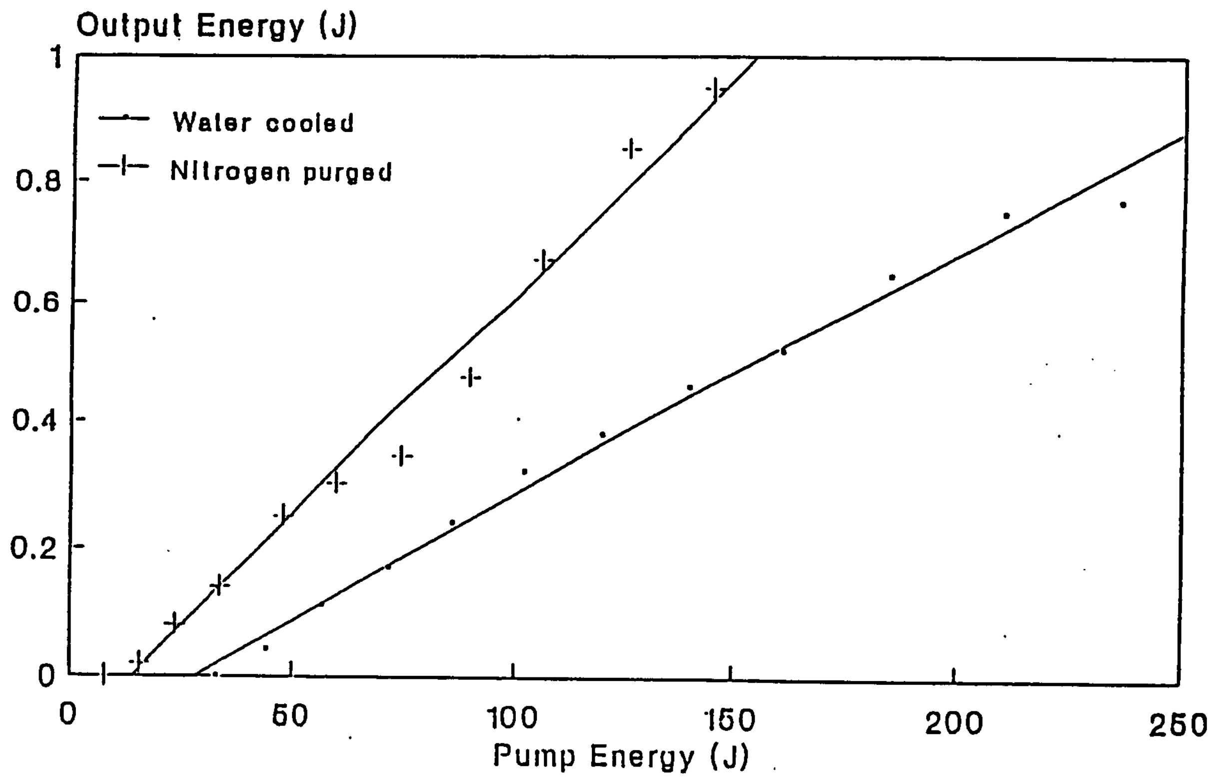

1 ms pulsewidth driver

October 22, 1991

FIGURE 6: Er, Cr, Yb:GLASS LASER PERFORMANCE

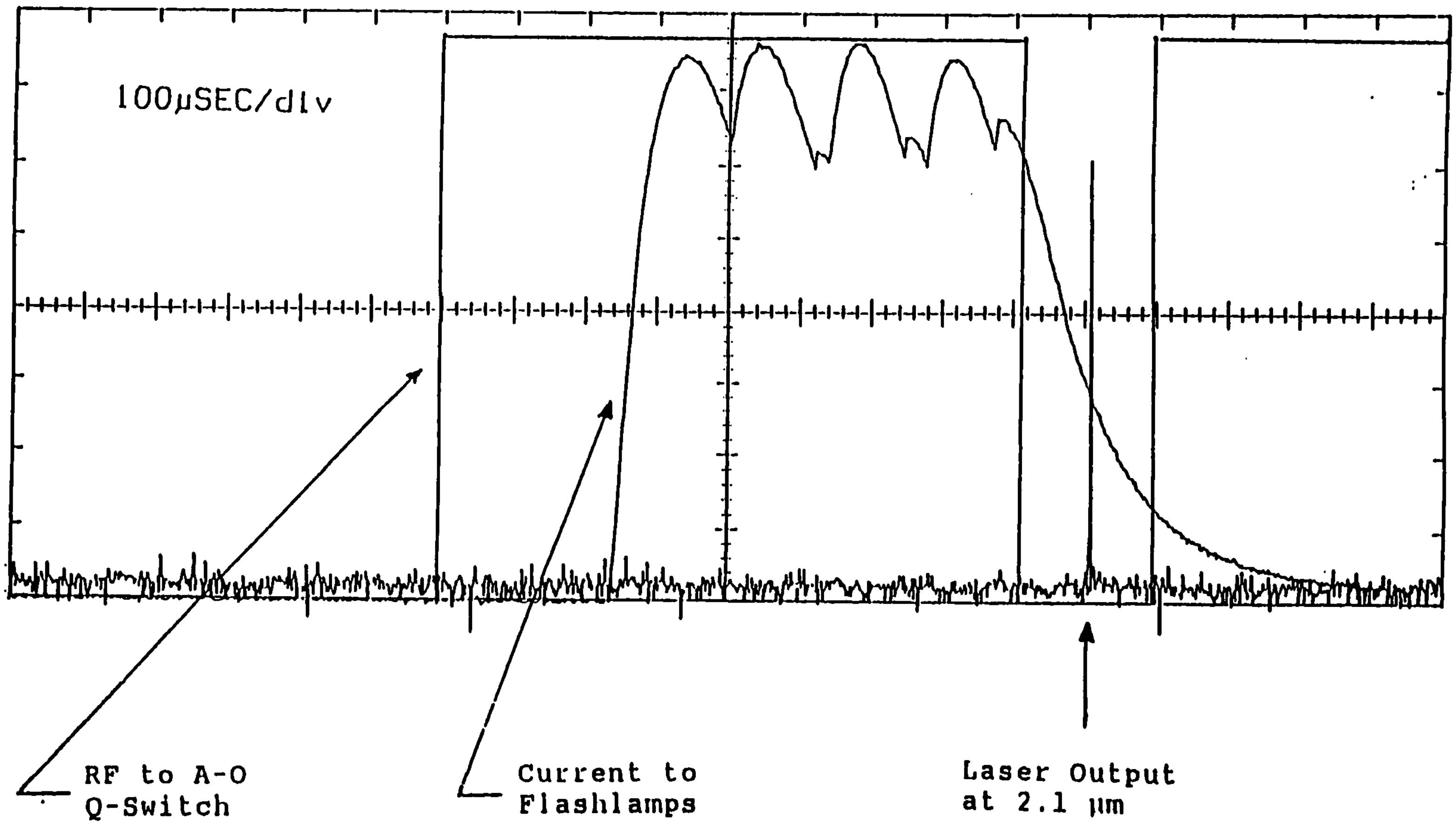

FIGURE 7: FLASHLAMP, RF, AND Q-SWITCH LASER PULSE FOR CTH:YAG

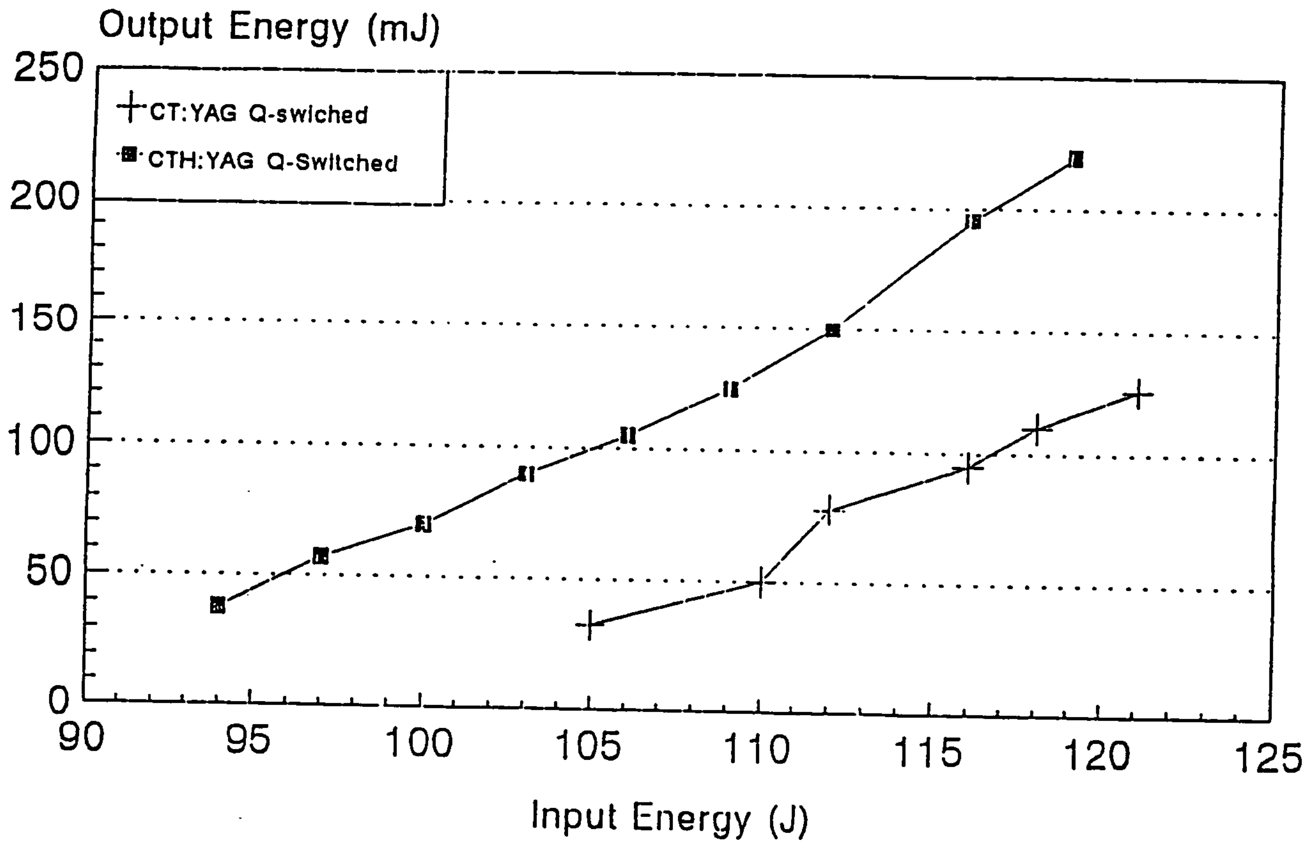

6.3mm diameter by 75mm long laser rods.

FIGURE 8: COMPARISON OF CT:YAG AND CTH:YAG LASERS

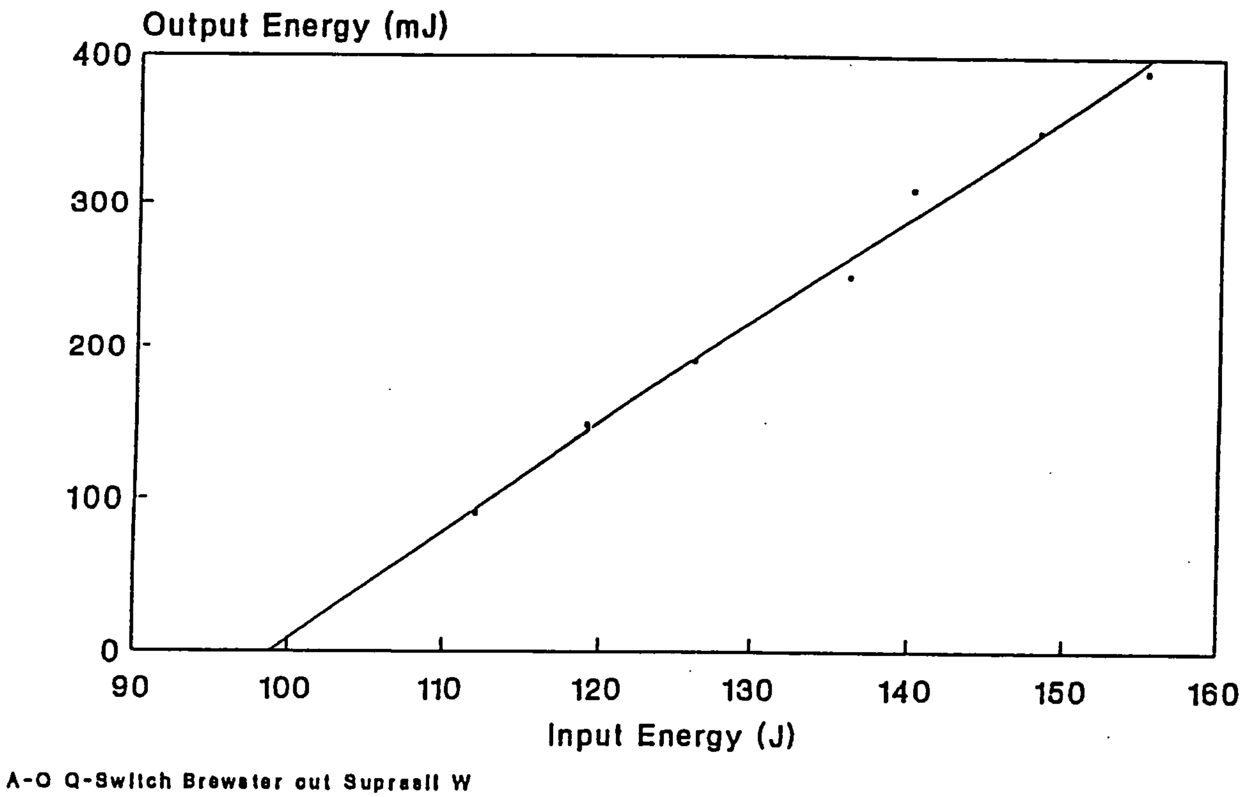

6.3mm diameter by 100mm long laser rod.

FIGURE 9: AO Q-SWITCH I/O DATA FOR CTH:YAG

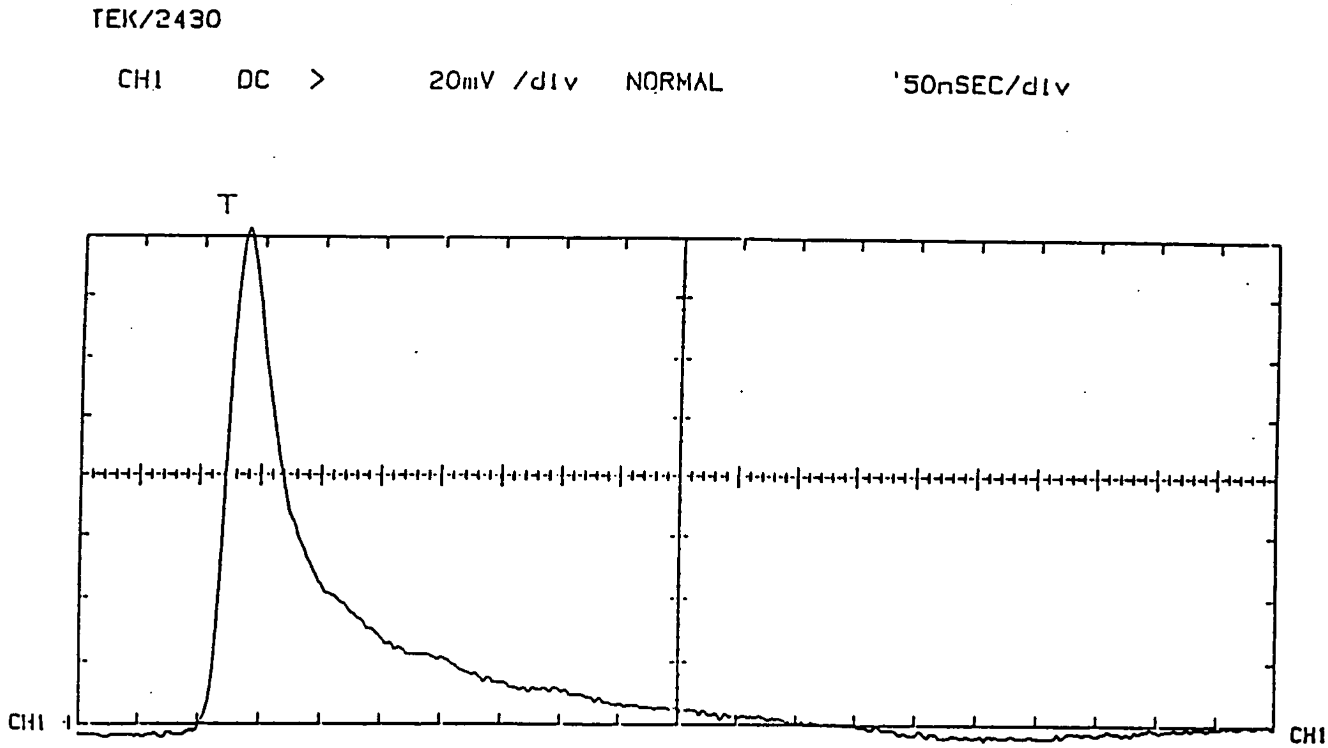

FIGURE 10: A/O Q-SWITCH LASER PULSE WIDTH, DATA FOR CTH:YAG

SECOND YEAR OF PHASE II PROGRAM

3.3 LASER CHARACTERIZATION AT USF

The following lasers were supplied by SEO to USF for their use in a lidar experimental set-up:

$Co:MgF_2$ laser: High output power in a non-Q-switched mode. However, significant laser cavity mirror damage was experienced when the laser was Q-switched at power levels greater than 50 mJ/pulse.

Ho:YAG laser: High output power in normal mode; limited to 300 mJ for Q-switched (but half of laser power was in a long tail); multiple wavelength operation (OK for aerosol Lidar).

Ho:YSGG laser: Lower in output power than Ho:YAG, but no multiple wavelength problems.

Tm:YAG/YLF laser: A low laser gain system more suited for CW operation. However, it would have significant utility if it could be diode laser pumped.

Er:YAG laser: High threshold system at room temperature; some significant up-conversion problems.

Of the above laser systems, the Ho:YAG seemed to be the most promising in terms of obtainable Q-switched laser operation. As such, the Ho:YAG laser was investigated the most and was used in the USF Lidar system. The basic results of the USF testing of the Ho:YAG laser (and of the Ho:YSGG) laser are given in the following sections. The basic testing of the $Co:MgF_2$ laser was reported in the final report of the Phase I SBIR program, and indicated that only low power (<50 mJ/pulse) output could be obtained when Q-switching due to optical damage limitations.

3.3.1 Ho:YAG LASER

The parameters for the Ho:YAG laser (and some associated lidar system characteristics) are given in Table II. It was found that close to half of the Ho:YAG laser output power fell within a long 200 μs tail, and could not be used for lidar measurements. As such, a 1 microsecond gate width was used in the A/O Q-switch to stop the laser tail from occurring. In addition, it was found that the laser operated on two lines at the same time. As such, intra-cavity etalons were used (0.2 and 0.5 mm thick) to control the operation of the lasers; see later sections.

The relative timing of the laser flashlamp and laser output is seen in Figure 11. The normal mode (non-Q-switched) pulse output occurs over a 0.5 ms time period, due to the length of the flashlamp output pulse and the slow energy transfer from the Tm to the Ho ions.

TABLE II

2.1 μm LIDAR PARAMETERS

* Direct Detection

* LASER:
  Cr:Tm:Ho:YAG @ $10^{\circ}C$
  Flash Lamp Pump
  100 W A/O Q-Switch
  2 Hz PRF
  Multimode

* LASER Power:
  750 mJ Normal Mode (No Q-Switch)
  ~ 300 mJ Q-Switched (but Half Power in 200 μS Tail)
  125 mJ Q-Switched (< 1 μS Pulse, but
  Multiple Wavelengths; 2.09 and 2.097 μm)
  With Etalons: 100 mJ (2 Lines) ; 50 mJ (1 Line)

* Telescope:
  40 cm Newtonian
  f = 180 cm
  FOV = 2 mrad.

* Detector:
  InSb @ 77K (or) InGaAs @ 243K

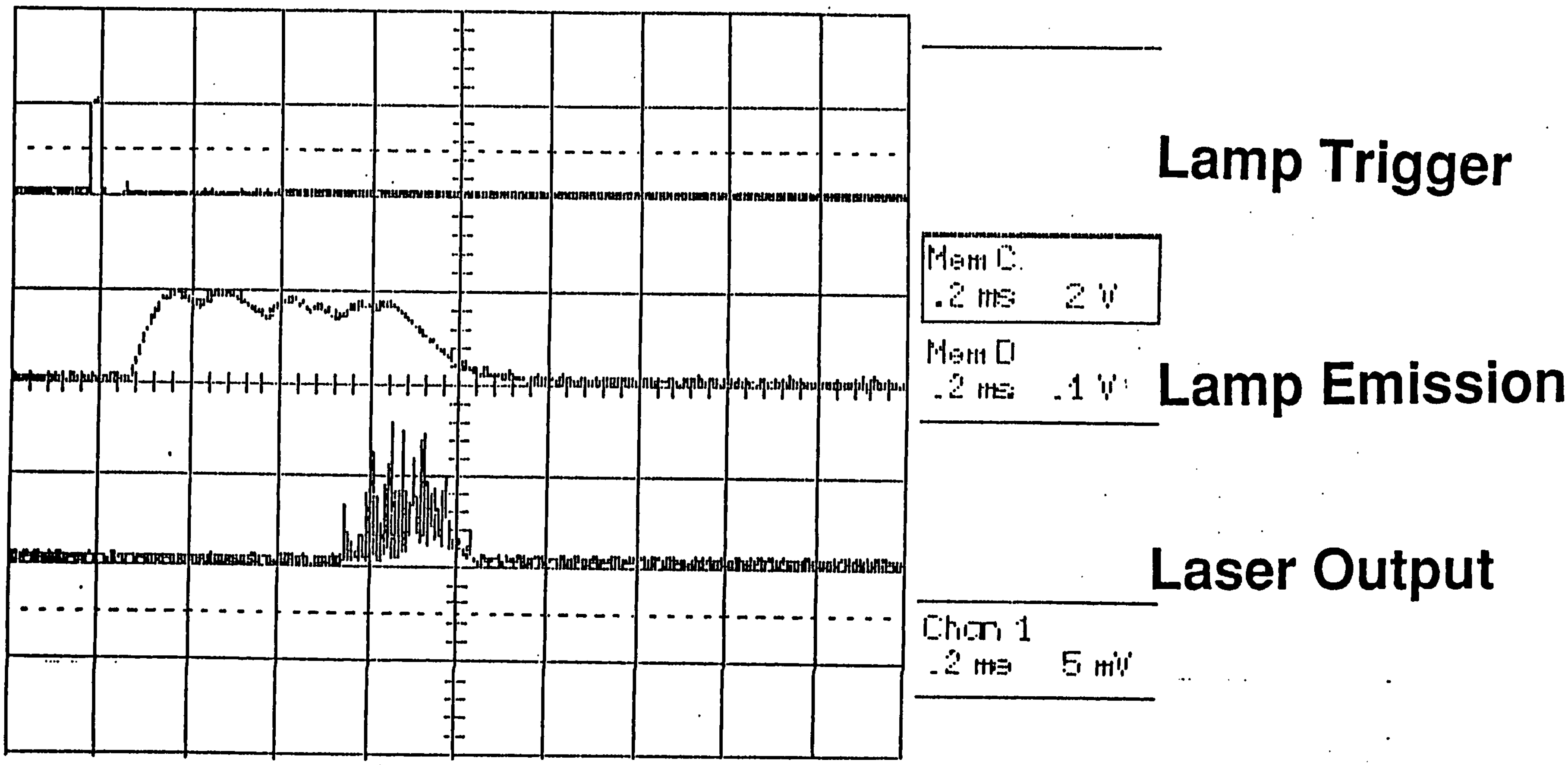

FIGURE 11: RELATIVE TIMING OF FLASHLAMP EMISSION AND Ho LASER OUTPUT
(NORMAL MODE, NO Q-SWITCH)

During the laboratory tests at USF and initial lidar atmospheric tests, it was determined that the Ho:YAG laser operates on two different lines or wavelengths simultaneously. As such, a spectrometer was used to separate out the different emission lines, and the temporal emission was recorded for each wavelength. Figure 12 shows the temporal emission at the two lines from the Ho:YAG laser. When the Ho:YAG laser was Q-switched, a similar behavior was observed as seen in Figure 13.

It was found that the degree of energy partitioned between the two emission wavelengths was a function of pump power and internal cavity loses. Figure 14 shows the relative output laser pulse as the pump energy into the flashlamp was changed. Figure 15 shows the measured spectral distribution of the Q-switched laser about the two laser emission lines. As seen, the lines are somewhat broad.

To reduce the effect of the two emission lines on an atmospheric lidar measurement, several different etalons were inserted into the laser cavity in order to establish the best selection of etalon thickness and number. It was found that 1 etalon (thickness 0.5 mm, uncoated quartz) would narrow the two lines considerably, but that both lines still lased. The use of two etalons (0.5 mm and 0.2 mm thick) narrowed the line even more and reduced the emission to one line. This is shown in Figure 16 which shows the spectrographic image of the Ho:YAG laser emission superimposed with the calculated transmission spectrum of the atmosphere for a path length of 5 km. Figure 17 shows the tuning range measured with the one etalon accomplished by tilting the angle of the etalon in the cavity.

Figure 18 shows the Ho:YAG laser emission lines measured by others superimposed on the calculated transmission spectrum of the atmosphere. As seen, each Ho line is actually composed of several splittings, each of almost similar gain characteristics. It is the presence of these similar split lines that appears to create the wide linewidth and mixed emission output of the Ho:YAG laser. As a result, future Ho:YAG laser design should most probably use a low-power oscillator followed by an injection seeded oscillator/amplifier combination.

3.4 LIDAR EXPERIMENTS

The Ho:YAG laser from SEO was incorporated into a lidar system. Figure 19 shows the Lidar system and the diagnostics used. The output from the laser was monitored with a power meter and peak sensing detectors, and spectrally observed in real-time with a spectrometer/IR video camera system. Most of the laser power was directed toward the outside atmosphere using Lidar steering mirrors. A photograph of the system is shown in Figure 20.

Initial lidar experiments were performed using the Ho:YAG laser and directing the beam in the vertical direction. Figure 21 shows the lidar signal obtained in this manner (Summer, 1992; high-humidity). Aerosol returns were measured out to a range of 5 to 6 km, and clouds were measured as shown. Figure 22 shows aerosol returns in a horizontal direction. Figure 23 shows returns from higher altitude clouds. These

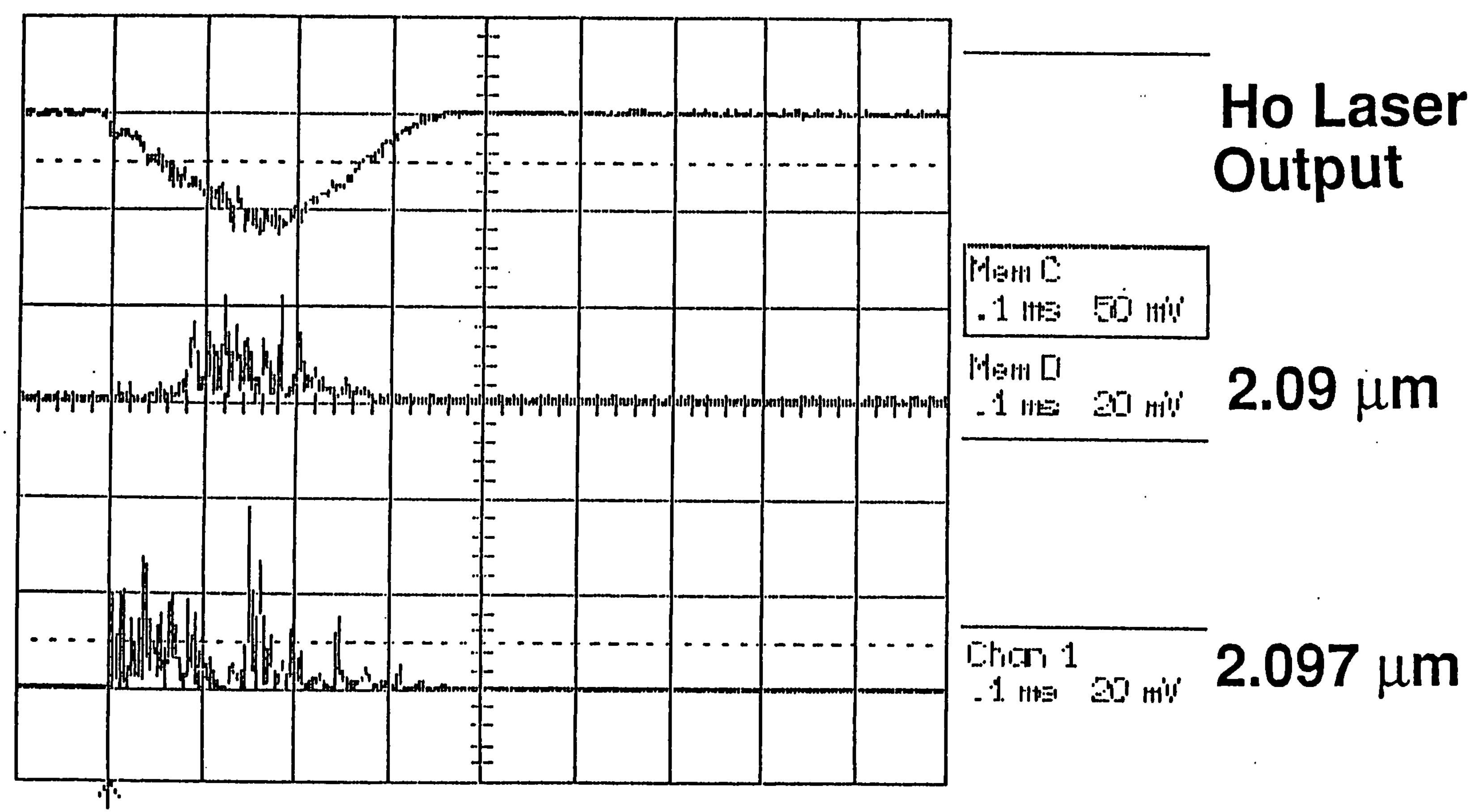

FIGURE 12: Ho LASER OUTPUT AT THE TWO DIFFERENT LASER LINES PRODUCED SIMULTANEOUSLY (NORMAL MODE, NO Q-SWITCH)

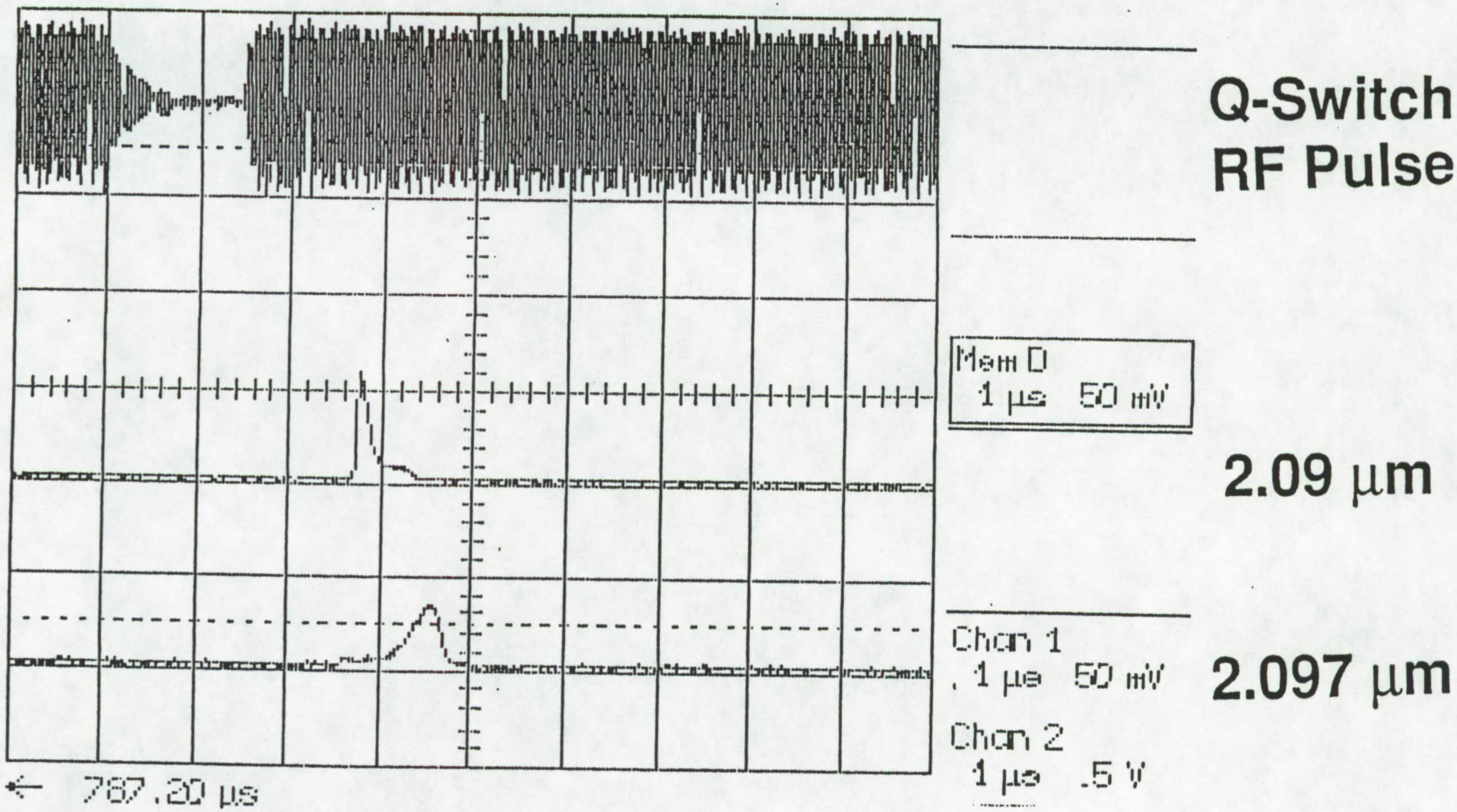

FIGURE 13: RELATIVE TIMING OF THE TWO Ho LASER WAVELENGTHS PRODUCED SIMULTANEOUSLY (Q-SWITCHED, 1 µS GATE)

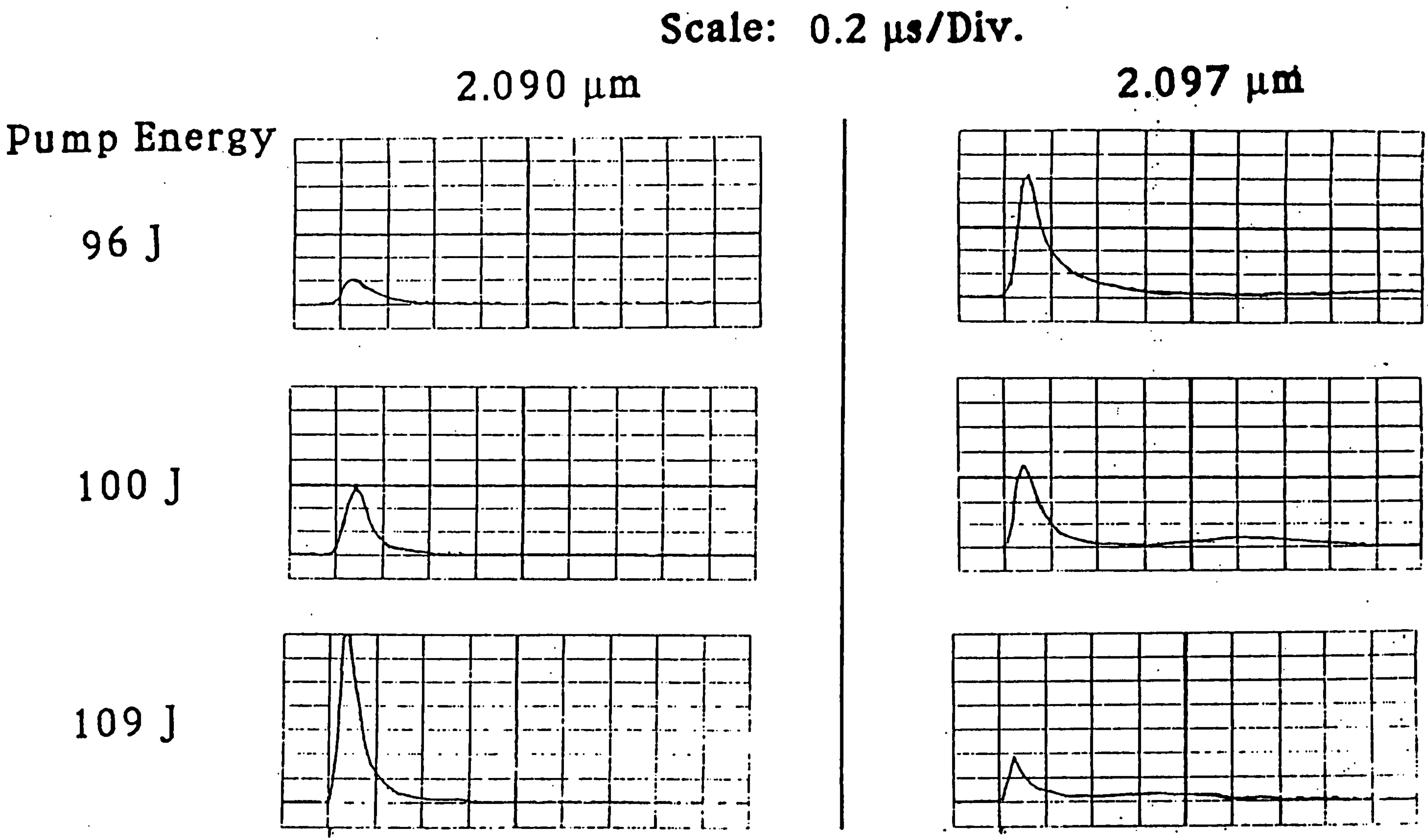

FIGURE 14: RELATIVE PULSE ENERGY VARIATION BETWEEN THE TWO LASING WAVELENGTHS 2.09 AND 2.097 µm AS A FUNCTION OF FLASHLAMP PUMP ENERGY (Q-SWITCHED)

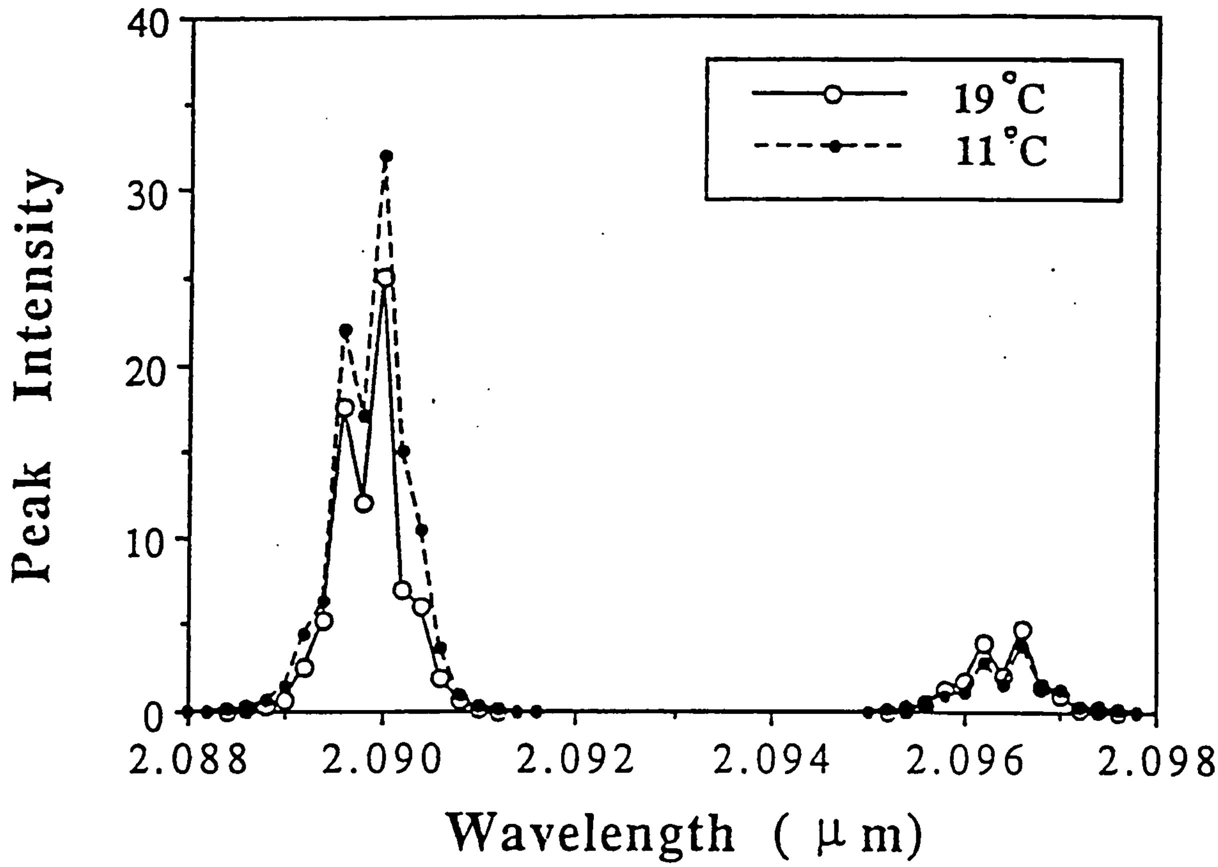

FIGURE 15: SPECTRAL DISTRIBUTION OF SINGLE Ho LASER PULSE (Q-SWITCHED)

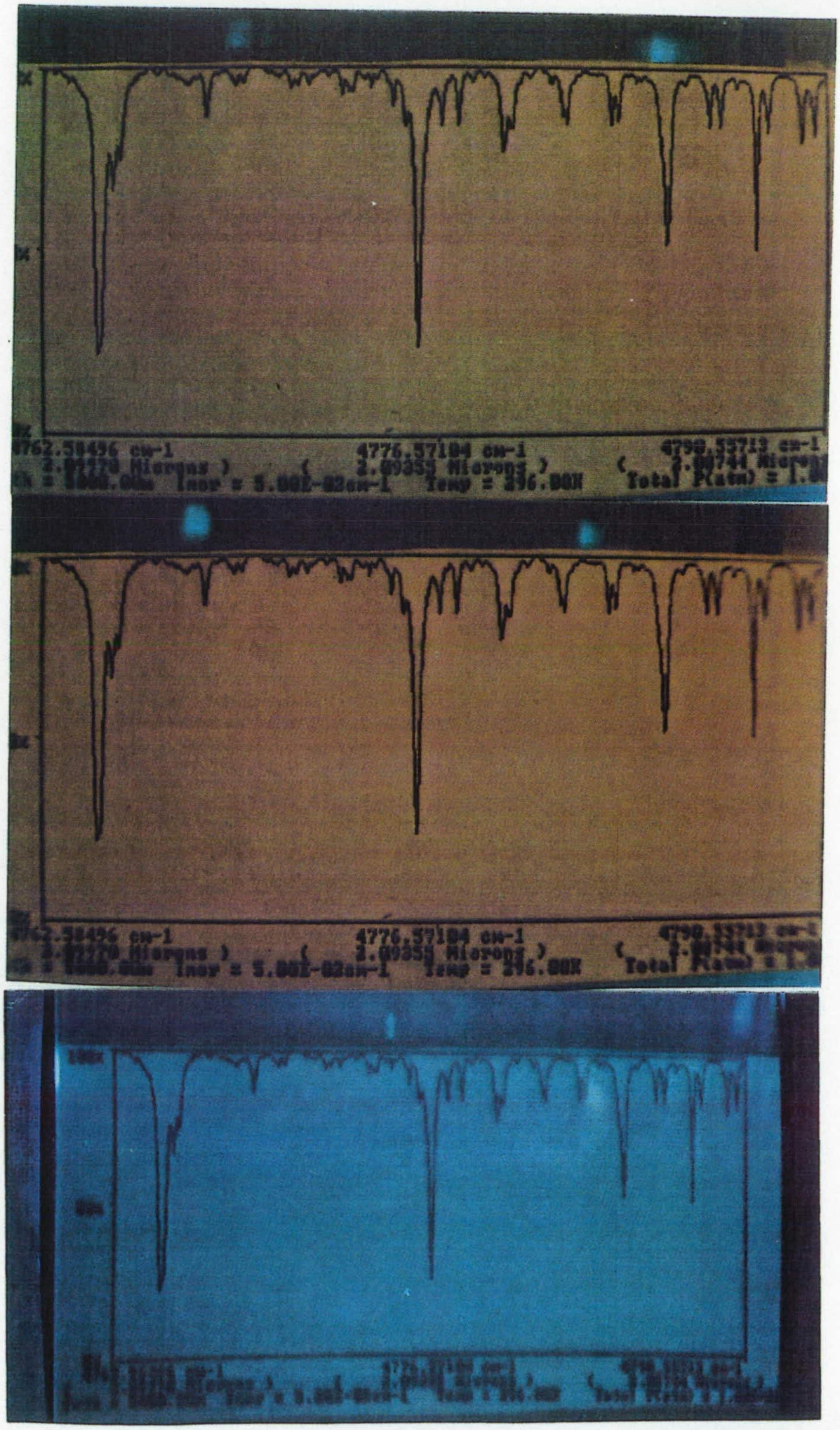

No Etalon

1 Etalon

2 Etalons

Photo of Spectrograph Image (Ho Laser Output) Superimposed on Atmospheric Transmission Spectra

FIGURE 16

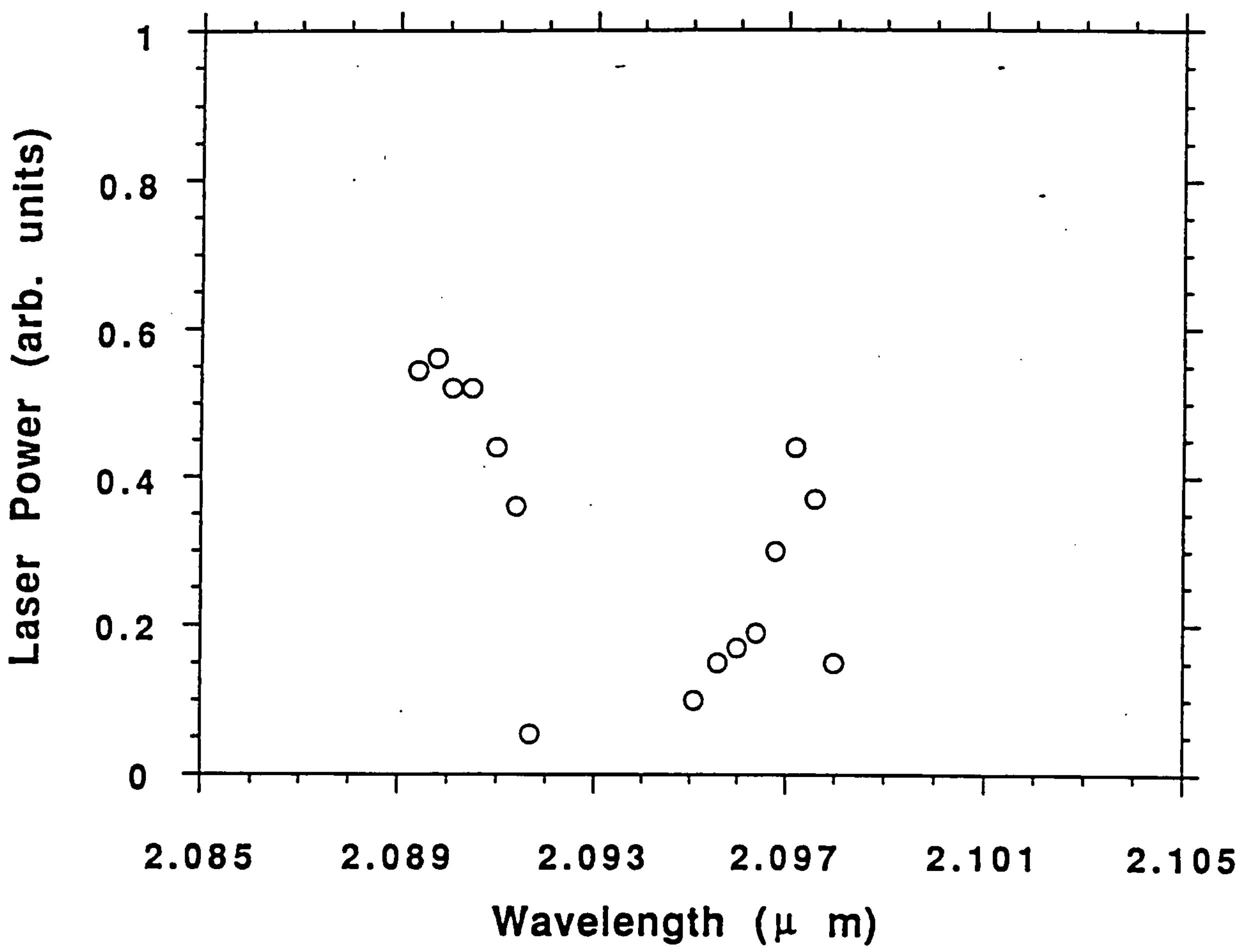

FIGURE 17: OUTPUT WAVELENGTH OF Ho;YAG LASER USING ONE INTRACAVITY ETALON (0.5 mm) FOR TUNING

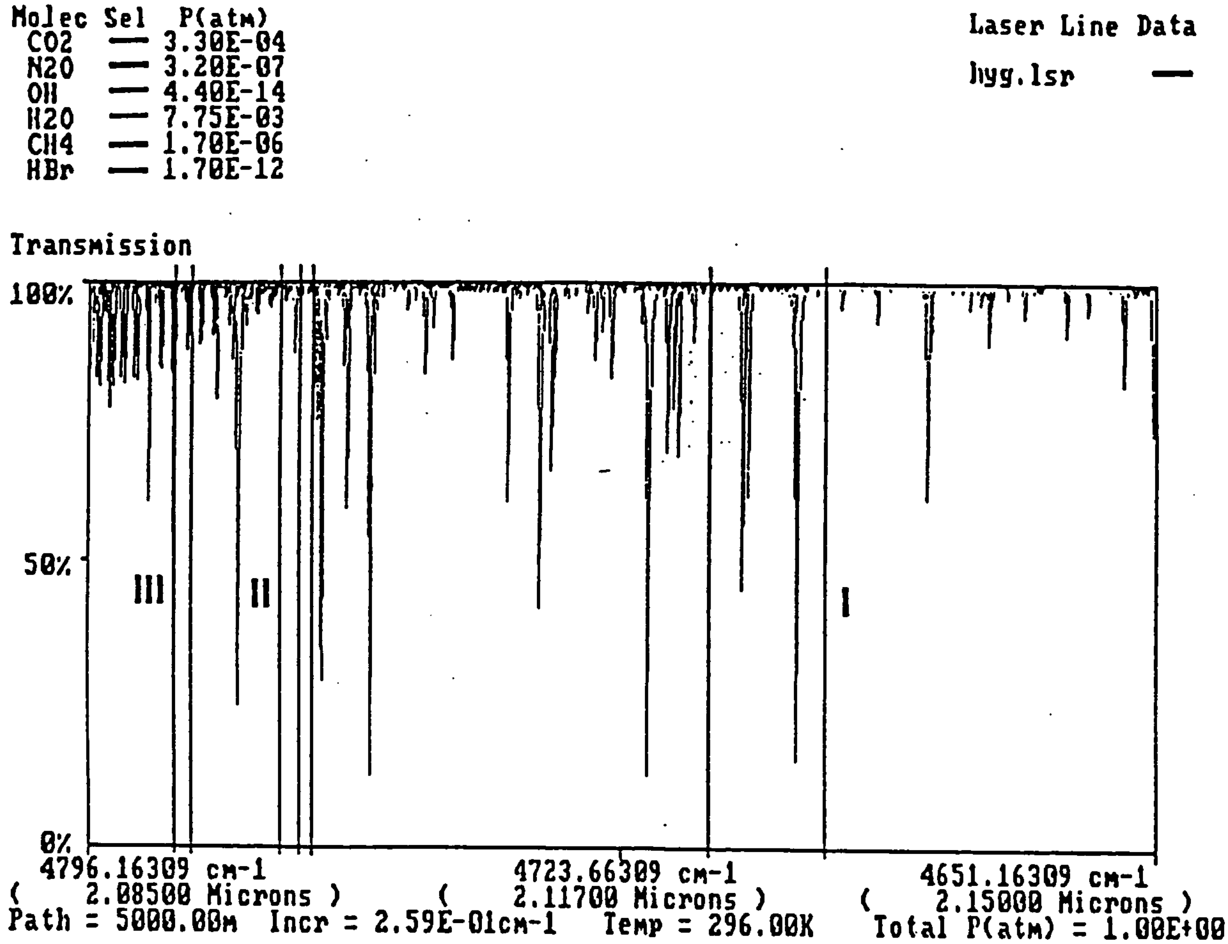

Ho:YAG Laser Emission Lines		
	Wavelength (µm)	Wavenumber (cm^{-1})
I	2.12952 2.12229	4695.9 4711.9
II	2.09824 2.09740 2.09630	4765.9 4767.8 4770.3
III	2.09110 2.09000	4782.2 4784.7

FIGURE 18: PREDICTED TRANSMISSION SPECTRUM OF ATMOSPHERE OVERLAYED WITH THE PREVIOUSLY MEASURED Ho:YAG LASER LINES

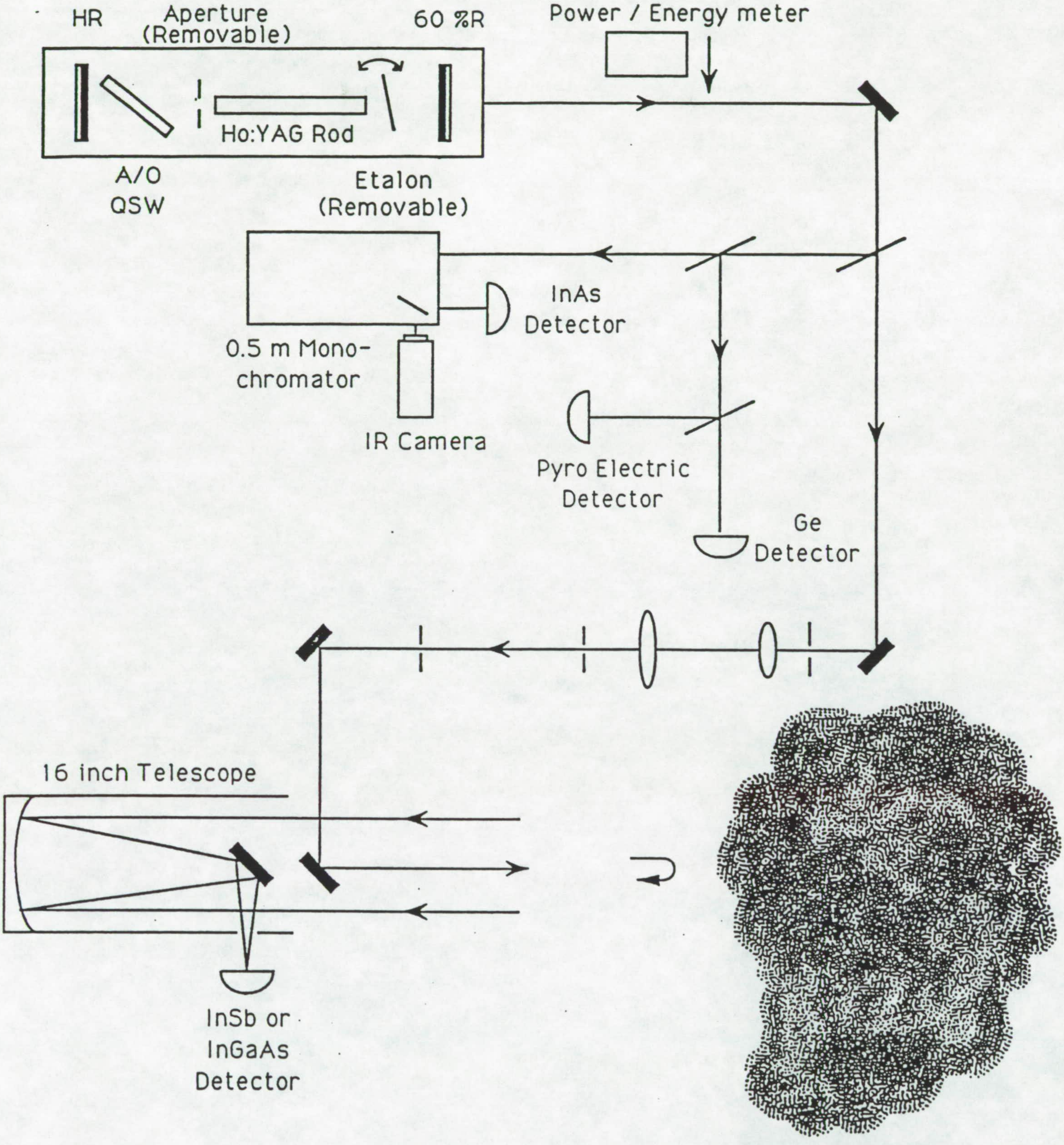

FIGURE 19: SCHEMATIC OF DIRECT DETECTION, HIGH POWER 2.1 μm Ho:YAG LIDAR SYSTEM FOR RANGE R/ESOLVED ATMOSPHERIC MEASUREMENTS

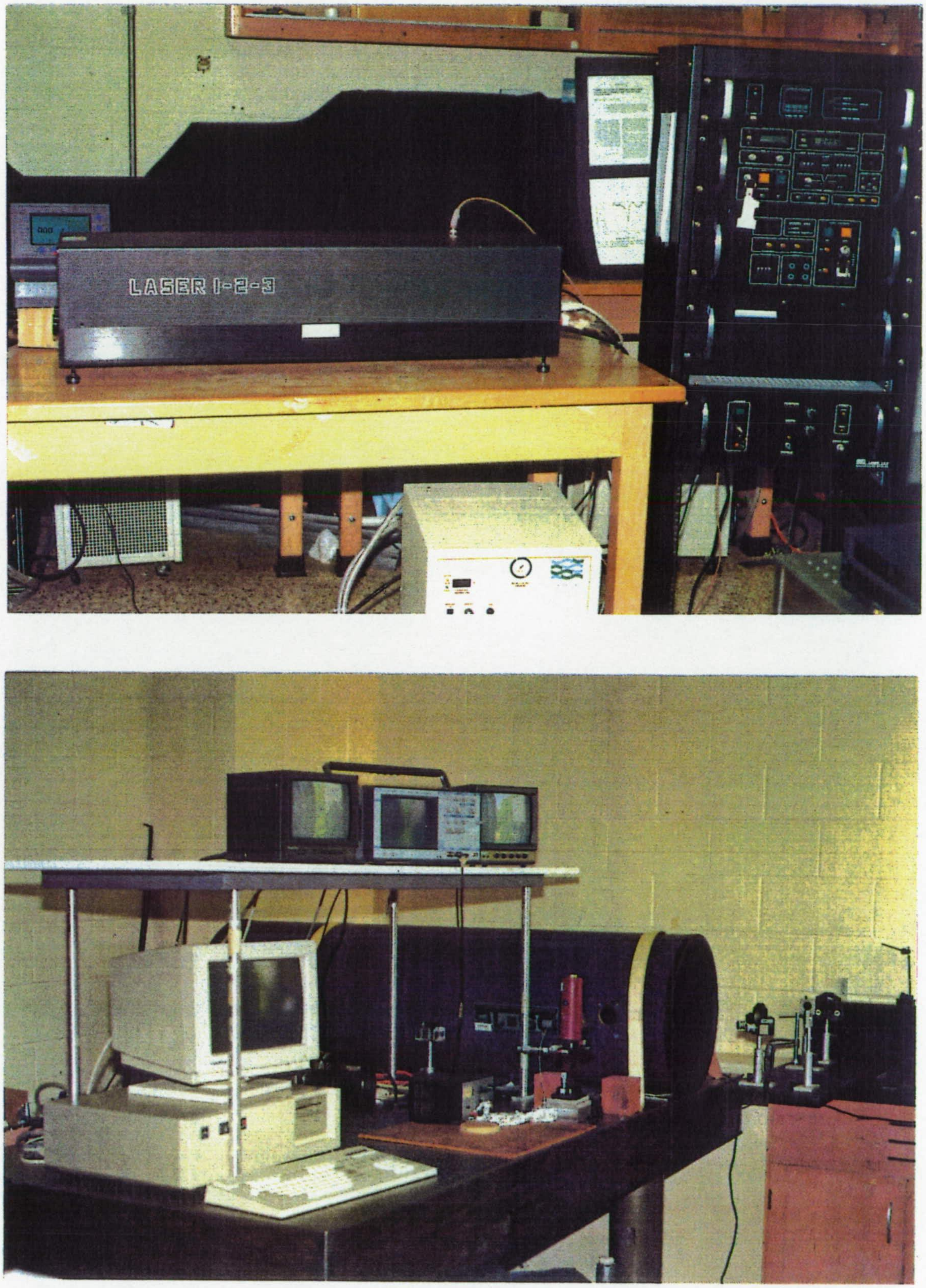

FIGURE 20: PHOTOGRAPH OF Ho:YAG LASER AND LIDAR TELESCOPE

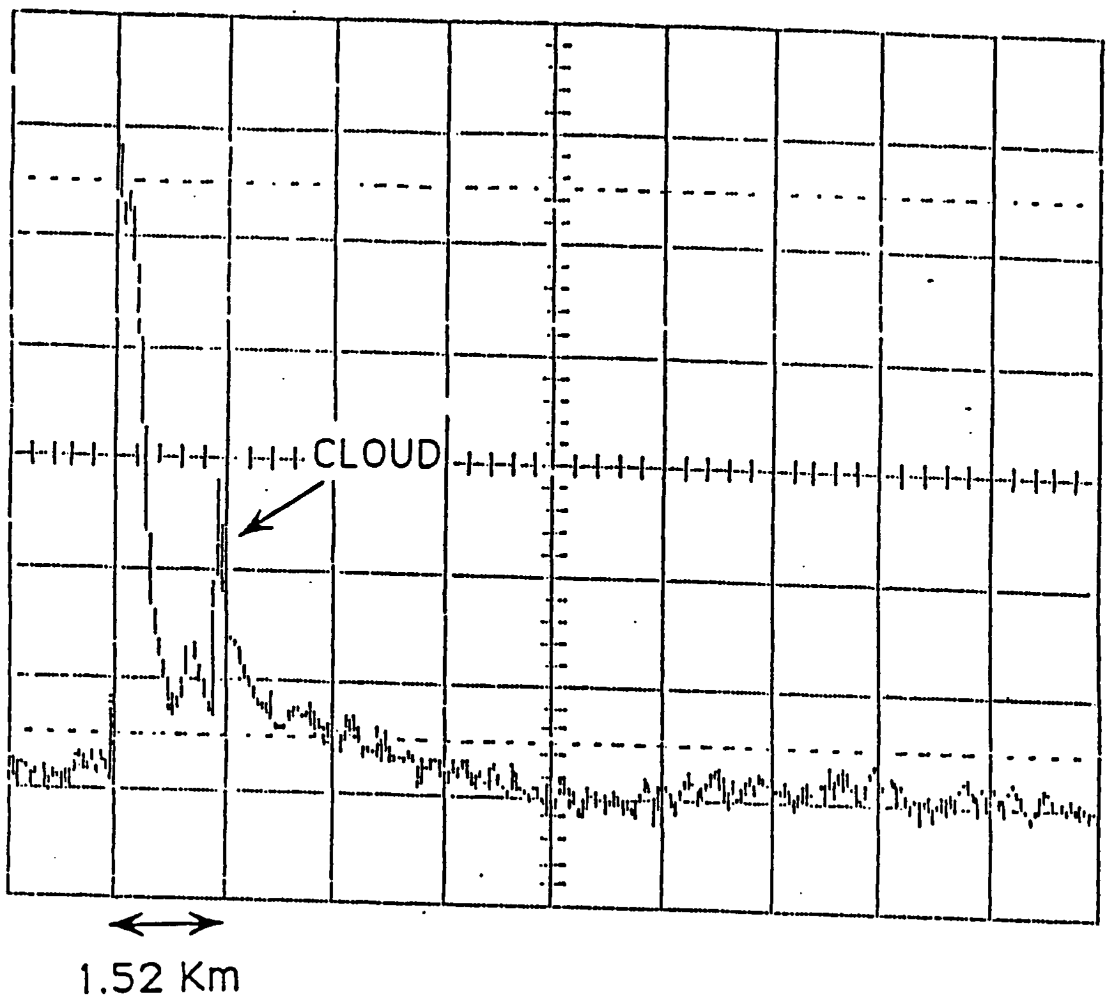

FIGURE 21: Ho LIDAR ATMOSPHERIC RETURN (VERTICAL DIRECTION)

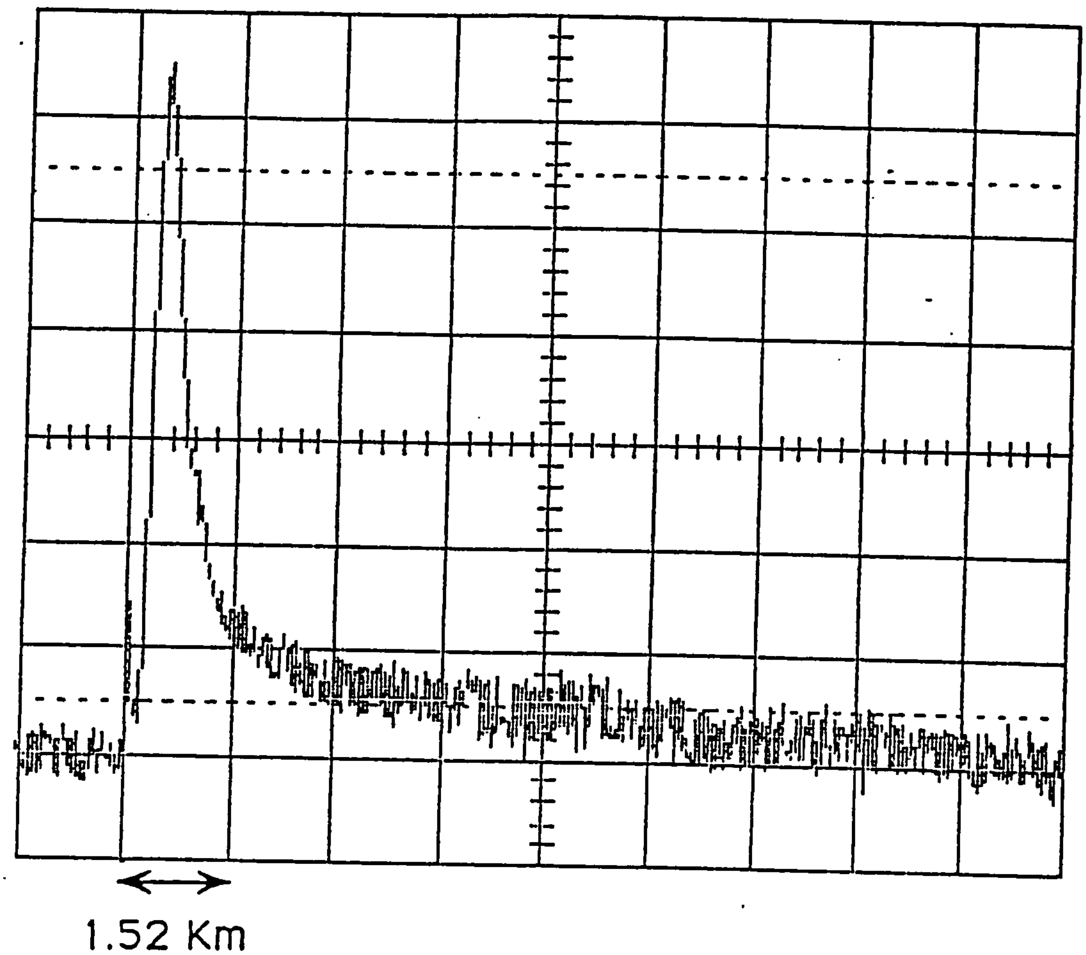

FIGURE 22: Ho LIDAR ATMOSPHERIC RETURN (HORIZONTAL DIRECTION)

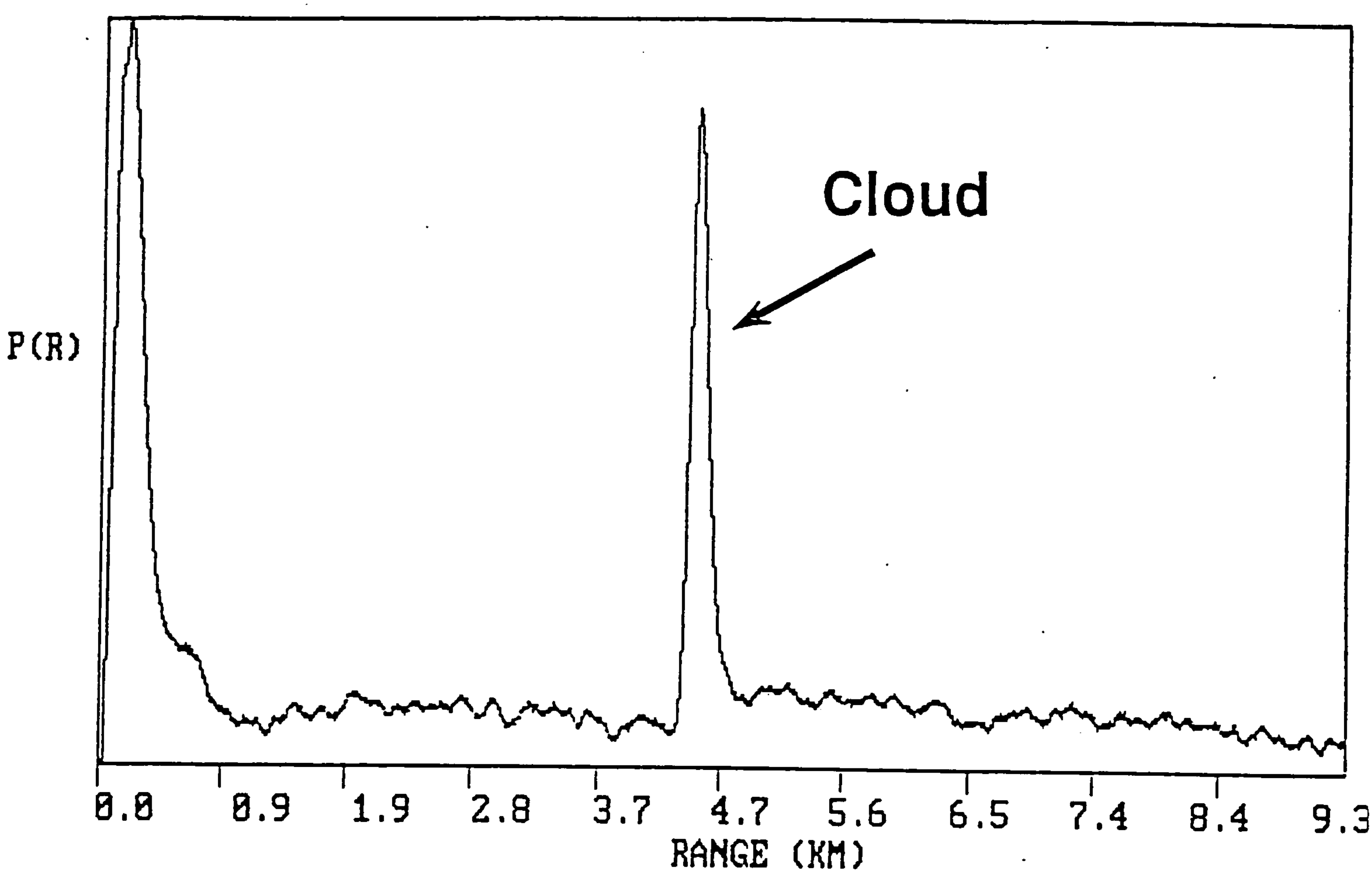

FIGURE 23: Ho LIDAR DETECTION OF CLOUD AT ALTITUDE OF 4.5 Km

experiments were obtained using a liquid nitrogen cooled InSb detector.

Figure 24 shows the DIAL measurements of water vapor in the atmosphere obtained by tuning the etalons in the Ho laser cavity.

3.4.1 LIQUID N_2 COOLED InSb VERSUS TE COOLED InGaAs PHOTODETECTOR

A TE cooled InGaAsP photodetector was also used with the Lidar measurements (Epitaxx photodetector 500TEGR22 with Analog Modules 710-159 2 MHz preamplifier). A comparison was made of this detector and the 1 mm diameter InSb detector. It was found that the two were essentially the same in S/N values for the Lidar returns. The TE cooled InGaAsP photodetector has the advantage that it does not have to be in a dewar or liquid N_2 cooled.

3.4.2 Ho:YAG VERSUS Ho:YSGG LASER

The Ho:YAG laser was also compared to the Ho:YSGG laser. Previous low-power laser/Lidar studies had indicated that the Ho:YSGG laser does not show multiple wavelengths when Q-switched. As a result, the Ho:YSGG laser module was used in the high power SEO laser, and the laser performance tested. It was found that the Ho:YSGG laser was about 50 mJ/pulse when it was Q-switched (and no etalons). This value is less than the value seen with the Ho:YAG cavity with etalons. As such, it was determined that the Ho:YAG was still the optimal choice, although further tests should still be conducted to better quantify this.

3.5 DELIVER LABORATORY BREADBOARD LIDAR COMPONENTS TO NASA

The lidar tests provided a data base for the design of an optimized Laboratory Breadboard lidar for atmospheric aerosol profiling. All the laser sources and the components developed for the lidar (transmitter/receiver optics, photodetector TE cooled InGaAsP) were delivered and installed at NASA LaRC by SEO and USF personnel. The list of the lidar components delivered is attached in Appendix A. Using these components an eye-safe, solid state aerosol profiling lidar that is easy to use can operated at NASA with a minimum of effort. The lidar signals will be analyzed by a computerized data acquisition system by NASA/LaRC providing significant new information.

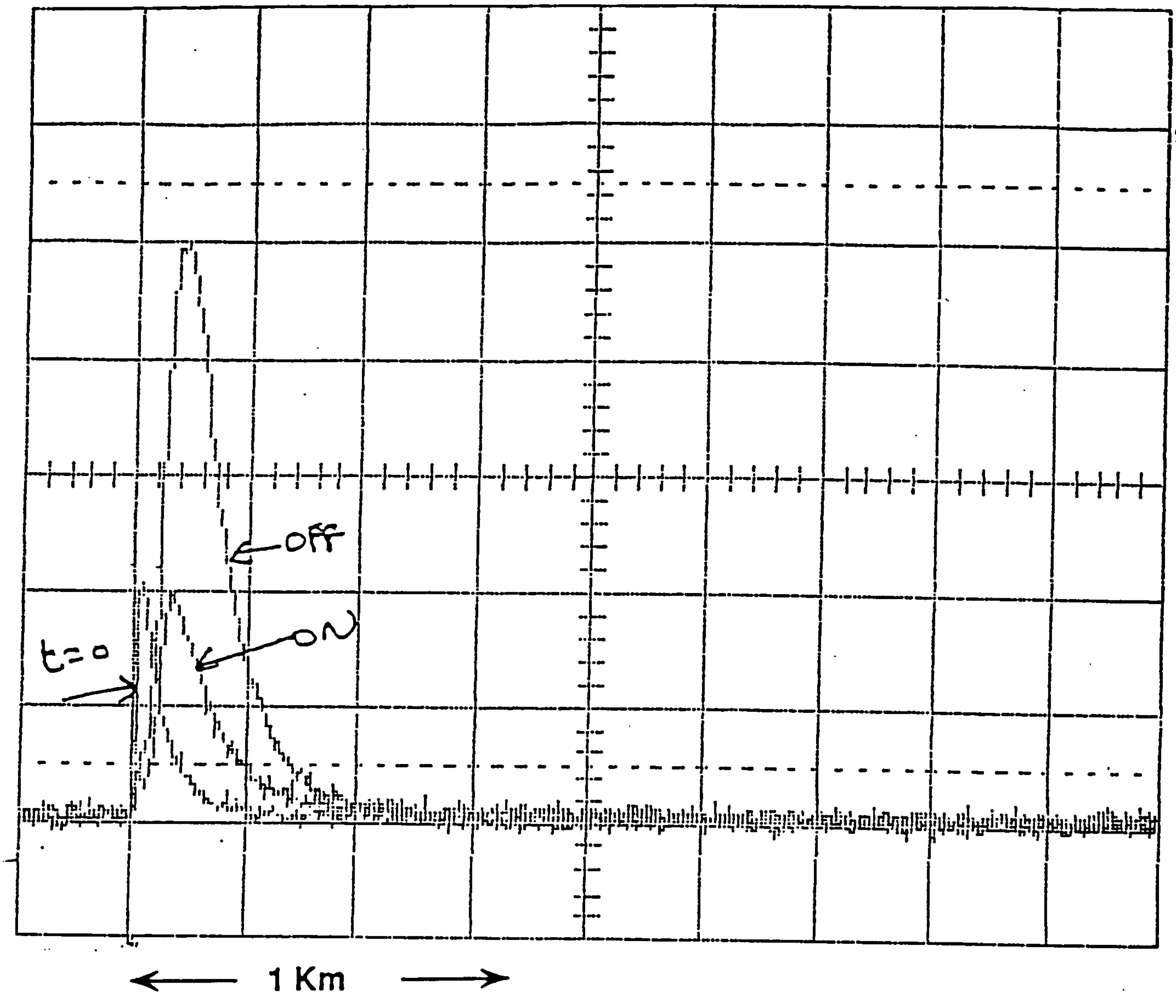

FIGURE 24: Ho LIDAR ATMOSPHERIC RETURNS AS Ho LASER WAS TUNED ON/OFF WATER VAPOR ABSORPTION LINE

4.0 CONCLUSIONS

A high power, multi-module, solid state laser was developed by SEO and studied to determine the optimal high-power eye-safe laser source for atmospheric lidar applications. Under this program, SEO developed and constructed a variety of flashlamp pumped solid-state lasers ($Co:MgF_2$ with 1.3 μm Nd:YAG pump, Ho:YSGG, Ho:YAG, Tm:YAG, and Er:Glass) which were tried as potential candidates for atmospheric lidar applications. The basic findings for the laser inter-comparison were:

$Co:MgF_2$ laser: High output power in a non-Q-switched mode. However, significant laser cavity mirror damage was experienced when the laser was Q-switched at power levels greater than 50 mJ/pulse using a Q-switch of material TeO_2.

Ho:YAG laser: High output power in normal mode; limited to 250 mJ for Q-switched (but half of the laser power was in the long tail); multiple wavelength operation (OK for aerosol lidar).

Ho:YSGG laser: Lower in output power than Ho:YAG, but no multiple wavelength problems.

Tm:YAG laser: A low laser gain system, however, it would have significant utility if it could be diode laser pumped due to its broad absorption pump line.

Er:Glass laser: High threshold system at room temperature; some significant up-conversion problems.

SEO developed these different lasers, and USF tested them as for their utility as a lidar source. After about a year of testing, it was determined that the optimal laser choice was the 2.1 μm Ho:YAG laser. The lidar data collected with the Ho:YAG laser indicated that the laser operates at two wavelengths 2.09 and 2.097 μm. The Ho lidar data presented in this report will provide baseline information on the use of Ho laser for atmospheric measurements.

All of the objectives of this SBIR Phase II program were accomplished. In addition, SEO was able to get two new products for commercial applications. These products include: (1) A room temperature tunable $Co:MgF_2$ laser providing up 200 mJ output energy, and (2) An AO Q-switch with Brewster's angle (without AR coatings) for Ho, Tm, and Er lasers.

5.0 REFERENCES

1. "Influence of Intrapulse Wavelength shifts of a high power Q-switched 2.1 m Ho:YAG laser on Atmospheric Lidar Measurements", M. Vaidyanathan, D.K. Killinger, M. Acharekar, and J. Montgomery, paper presented at CLEO '93 Baltimore.

2. "Eye-Safe 2.1 μm Ho Lidar for measuring atmospheric density profiles", N. Sugimot, N. Simms, K. Chan, and D.K. Killinger, Optics Letters 15, 302 (1990).

3. "Investigation of 2.1 μm lasing properties of Ho:TM:Cr:YAG crystals under flashlamp pumping a various operating conditions", K. Kim, Y. Choi, N. Barnes, R. Hess, C. Blair, and P. Brockman, Applied Optics 32, 2066 (1993).

4. "Laser and spectral properties of Cr, Tm, Ho:YAG at 2.1 μm", S. Bowman, M. Winings, R. Auyeung, J. Tucker, S. Searles, and B. Feldman, IEEE J. of Quant. Elect. 27, 2142 (1991).

5. "Spectroscopy and Diode laser pumped operation of Tm, Ho:YAG", T.Y. Fan, G. Huber, R. Byer, and P. Mitzscherlich, IEEE J. of Quant. Elect. 24, 924 (1988).

APPENDIX A

LIST OF COMPONENTS DELIVERED TO NASA LaRC

LIST OF COMPONENTS DELIVERED TO NASA LaRC

ITEM	DESCRIPTION	UNITS
1	SEO Laser 1-2-3 with CTH:YSGG Module, HR @ 2.1 μm, 60%R @ 2.1 μm, A/O Q-Switch	1
2	SEO A/O Q-Switch Driver, Model A-O, S/N 001	1
3	SEO Laser 1-2-3 Power Supply, Model 882-1-6-C, S/N 91040303	1
4	SEO Laser Power Supply Controller, Model 880-5/1, S/N 90022705	1
5	SEO Pulse Forming Network, Model 880-5/2, S/N 90022810	1
6	SEO Co:MgF_2 Laser Gas Purge and TE Cooler Controller	1
7	SEO Rack Cart	1
8	SEO CTH:YAG Laser Module	1
9	SEO CT:YAG Laser Module	1
10	SEO Er:Glass Laser Module	1
11	SEO 1.32 m Nd:YAG Laser Module, HR @ 1.32 μm on a Mount, OC Mirror @ 1.32 μm Focussing Optics	1
12	SEO CTH:YAG Laser Mirrors 60%R, 2'-3' wedge, AR @ 2.1 μm 60%R, Flat/Flat, AR @ 2.1 μm 70%R, Flat/Flat, AR @ 2.1 μm 75%R, Flat/Flat, AR Coated HR and 60%R Set, Flat/Flat AR Coated	 1 2 1 1 2
13	Detector/Amplifier Units Epitaxx InGaAs (Red Extended) Detector Model 500TEGR22, S/N 9147EO917 with Analog Modules Amplifier Model 710-159, S/N 93031116; USF #4950-00187602 Epitaxx InGaAs (Red Extended) Detector Model 500TEGR22, S/N 9147EO920 with Analog Modules Amplifier Model 710-159, S/N 930311115, USF #4950-00187603	 1 1
14	Virgo Optics Beam Expander Kit FL = 100 mm, 1" dia, PLCC Lens AR @ 2.1 μm FL = 500 mm, 2" dia, PLCX Lens, AR @ 2.1 μm	1

REPORT DOCUMENTATION PAGE

Form Approved
OMB No. 0704-0188

1. AGENCY USE ONLY *(Leave blank)*

2. REPORT DATE
September 1993

3. REPORT TYPE AND DATES COVERED
Contractor Report

4. TITLE AND SUBTITLE
Novel $Co:MgF_2$ Lidar for Aerosol Profiler

5. FUNDING NUMBERS
C NAS1-19300

6. AUTHOR(S)
M.A. Acharekar

7. PERFORMING ORGANIZATION NAME(S) AND ADDRESS(ES)
Schwartz Electro-optics, Inc.
3404 N. Orange Blossom Trail
Orlando, FL 32804

8. PERFORMING ORGANIZATION REPORT NUMBER
C1413FNL.RPT

9. SPONSORING/MONITORING AGENCY NAME(S) AND ADDRESS(ES)
National Aeronautics and Space Administration
Langley Research Center
Hampton, VA 23665-5225

10. SPONSORING/MONITORING AGENCY REPORT NUMBER
NASA CR191525

11. SUPPLEMENTARY NOTES
Langley Technical Monitor: Dr. David M. Winker
Final Report

12a. DISTRIBUTION/AVAILABILITY STATEMENT
Unclassified - Unlimited

12b. DISTRIBUTION CODE

13. ABSTRACT *(Maximum 200 words)*

Lidars are of great interest because of their unique capabilities in remote sensing applications in sounding of the atmosphere, meteor-ology, and climatology. In this small business innovative research (SBIR) phase II program, laser sources including $Co:MgF_2$, CTH:YAG, CTH:YSGG, CT:YAG, and Er:Glass were evaluated. Modulator of fused silica and TeO_2 materials with Brewster's angle end faces were used with these lasers as acousto-optical (AO) Q-switches. A higher hold-off energy and hence a higher Q-switched energy was obtained by using a high power RF driver. The report provides performance characteristics of these lasers. The tunable (1.75-2.50 μm) $Co:MgF_2$ laser damaged the TeO_2 Q-switch cell. However, the CTH:YAG laser operating at 2.09 μm provided output energy of over 300 mJ/p in 50 ns pulse width using the fused silica Q-switch. This Q-switched CTH:YAG laser was used in a breadboard vertical aerosol profiler. A 40 cm diameter telescope, InSb and InGaAs detectors were used in the receiver. The data obtained using this lidar is provided in the report. The data shows that the eye safe lidar using CTH:YAG laser for the vertical aerosol density and range measurements is the viable approach.

14. SUBJECT TERMS
Lidar, Aerosol Profiler, Tunable Laser

15. NUMBER OF PAGES
43

16. PRICE CODE

17. SECURITY CLASSIFICATION OF REPORT	18. SECURITY CLASSIFICATION OF THIS PAGE	19. SECURITY CLASSIFICATION OF ABSTRACT	20. LIMITATION OF ABSTRACT
Unclassified	Unclassified		